

**COPY 1**  
DOT/FAA/PM-86/26

Program Engineering  
and Maintenance Service  
Washington, D.C. 20591

FAA WJH Technical Center  
00093123

**FEDERAL AVIATION ADMINISTRATION**

**SEP 30 1986**

**TECHNICAL CENTER LIBRARY  
ATLANTIC CITY, N.J. 08405**

# Field Performance of Fiber-Reinforced Concrete Airfield Pavements

Raymond S. Rollings

Geotechnical Laboratory  
DEPARTMENT OF THE ARMY  
Waterways Experiment Station  
Corps of Engineers  
Vicksburg, Mississippi 39180

July 1986  
Final Report

This Document is available to the public through the National Technical Information Service, Springfield, Virginia 22161.

FAA WJH Technical Center  
Tech Center Library  
Atlantic City, NJ 08405

**AVAILABLE IN  
ELECTRONIC FORMAT**



U.S. Department of Transportation  
**Federal Aviation Administration**

## NOTICE

This document is disseminated under the sponsorship of the Department of Transportation in the interest of information exchange. The United States Government assumes no liability for its contents or use thereof.

The United States Government does not endorse products of manufacturers. Trade or manufacturers' names appear herein solely because they are considered essential to the object of this report.

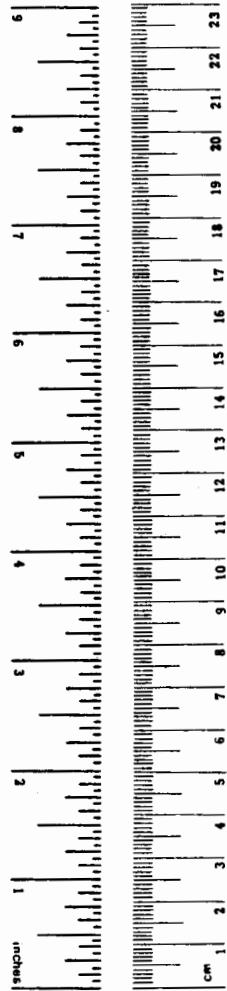
1. Report No. DOT/FAA/PM-86/26	2. Government Accession No.	3. Recipient's Catalog No.	
4. Title and Subtitle FIELD PERFORMANCE OF FIBER-REINFORCED CONCRETE AIRFIELD PAVEMENTS		5. Report Date July 1986	6. Performing Organization Code
7. Author(s) Raymond S. Rollings		8. Performing Organization Report No. WES TR GL-86-11	
9. Performing Organization Name and Address US Army Engineer Waterways Experiment Station Geotechnical Laboratory PO Box 631, Vicksburg, MS 39180-0631		10. Work Unit No. (TRAIS)	11. Contract or Grant No.
12. Sponsoring Agency Name and Address US Army Corps of Engineers and US Department of Transportation Federal Aviation Administration Washington, DC 20591		13. Type of Report and Period Covered Final Report January 1983-January 1985	
15. Supplementary Notes The US Army Engineer Waterways Experiment Station conducted this study jointly sponsored by the US Army Corps of Engineers and the Federal Aviation Administration under Inter-Agency Agreement No. DTFA01-83-Y-30606.		14. Sponsoring Agency Code APM-740	
16. Abstract <p>A field survey of steel fiber-reinforced concrete airfield pavements found the most serious performance problem to be permanent, early age curl of slabs and associated cracking. An examination of possible causes of this curl indicates it is probably due to the use of large slabs and thin sections. This study recommends slab sizes which should minimize this problem in the future. Other identified performance problems unique to this type pavement include loose surface fibers and nonfunctioning contraction joints.</p> <p>The design criteria for fiber-reinforced concrete were reviewed, and new criteria are proposed that are compatible with the Corps of Engineers change in portland cement concrete design criteria. A new method of overlay design was also proposed.</p>			
17. Key Words Curling Fiber-reinforced concrete Pavement design Pavement performance Pavements		18. Distribution Statement This document is available to the public through the National Technical Information Service, Springfield, Virginia 22161.	
19. Security Classif. (of this report) Unclassified	20. Security Classif. (of this page) Unclassified	21. No. of Pages 50	22. Price

## METRIC CONVERSION FACTORS

### Approximate Conversions to Metric Measures

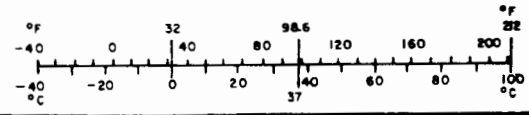
Symbol	When You Know	Multiply by	To Find	Symbol
<b>LENGTH</b>				
in	inches	2.5	centimeters	cm
ft	feet	30	centimeters	cm
yd	yards	0.9	meters	m
mi	miles	1.6	kilometers	km
<b>AREA</b>				
in <sup>2</sup>	square inches	6.5	square centimeters	cm <sup>2</sup>
ft <sup>2</sup>	square feet	0.09	square meters	m <sup>2</sup>
yd <sup>2</sup>	square yards	0.8	square meters	m <sup>2</sup>
mi <sup>2</sup>	square miles	2.6	square kilometers	km <sup>2</sup>
	acres	0.4	hectares	ha
<b>MASS (weight)</b>				
oz	ounces	28	grams	g
lb	pounds	0.45	kilograms	kg
	short tons (2000 lb)	0.9	tonnes	t
<b>VOLUME</b>				
tsp	teaspoons	5	milliliters	ml
Tbsp	tablespoons	15	milliliters	ml
fl oz	fluid ounces	30	milliliters	ml
c	cups	0.24	liters	l
pt	pints	0.47	liters	l
qt	quarts	0.95	liters	l
gal	gallons	3.8	liters	l
ft <sup>3</sup>	cubic feet	0.03	cubic meters	m <sup>3</sup>
yd <sup>3</sup>	cubic yards	0.76	cubic meters	m <sup>3</sup>
<b>TEMPERATURE (exact)</b>				
°F	Fahrenheit temperature	5/9 (after subtracting 32)	Celsius temperature	°C

\* 1 in. = 2.54 (exactly). For other exact conversions and more detailed tables, see NBC Misc. Publ. 286, Units of Weights and Measures, Price \$2.25, SD Catalog No. C13.10:286.



### Approximate Conversions to Metric Measures

Symbol	When You Know	Multiply by	To Find	Symbol
<b>LENGTH</b>				
mm	millimeters	0.04	inches	in
cm	centimeters	0.4	inches	in
m	meters	3.3	feet	ft
m	meters	1.1	yards	yd
km	kilometers	0.6	miles	mi
<b>AREA</b>				
cm <sup>2</sup>	square centimeters	0.16	square inches	in <sup>2</sup>
m <sup>2</sup>	square meters	1.2	square yards	yd <sup>2</sup>
km <sup>2</sup>	square kilometers	0.4	square miles	mi <sup>2</sup>
ha	hectares (10,000 m <sup>2</sup> )	2.5	acres	
<b>MASS (weight)</b>				
g	grams	0.035	ounces	oz
kg	kilograms	2.2	pounds	lb
t	tonnes (1000 kg)	1.1	short tons	
<b>VOLUME</b>				
ml	milliliters	0.03	fluid ounces	fl oz
l	liters	2.1	pints	pt
l	liters	1.06	quarts	qt
l	liters	0.26	gallons	gal
m <sup>3</sup>	cubic meters	35	cubic feet	ft <sup>3</sup>
m <sup>3</sup>	cubic meters	1.3	cubic yards	yd <sup>3</sup>
<b>TEMPERATURE (exact)</b>				
°C	Celsius temperature	9/5 (then add 32)	Fahrenheit temperature	°F



## PREFACE

The study described herein was sponsored by the Office, Chief of Engineers, as a part of the Facilities Investigation and Studies Program and by the Federal Aviation Administration as part of Inter-Agency Agreement No. DTFA01-83-Y-30606 Advanced Construction Procedure. The fieldwork was performed from January 1983 to January 1985.

The investigation for this study was conducted at the US Army Engineer Waterways Experiment Station (WES) under the general supervision of Mr. H. H. Ulery, Chief, Pavement Systems Division, and Dr. W. F. Marcuson, Chief, Geotechnical Laboratory. Mr. R. S. Rollings prepared the report. The report was edited by Ms. Odell F. Allen, Information Products Division, Information Technology Laboratory.

Director of WES during the preparation and publication of this report was COL Allen F. Grum, USA. Technical Director was Dr. Robert W. Whalin.

## CONTENTS

	<u>Page</u>
INTRODUCTION.....	1
BACKGROUND.....	1
SCOPE.....	1
FIELD SURVEY.....	2
INTRODUCTION.....	2
NORFOLK NAVAL AIR STATION, VIRGINIA.....	2
FALLON NAVAL AIR STATION, NEVADA.....	3
TAMPA INTERNATIONAL AIRPORT.....	7
McCARRAN INTERNATIONAL AIRPORT.....	7
CANNON AIRPORT.....	12
SALT LAKE CITY INTERNATIONAL AIRPORT.....	14
STAPLETON AIRPORT.....	14
ANALYSIS OF FIELD PROBLEMS.....	16
CURLING.....	16
SHRINKAGE.....	18
SHRINKAGE CALCULATION.....	20
VOLUME CHANGE MECHANISMS.....	22
APPROACHES TO CURLING PROBLEM.....	22
JOINT PERFORMANCE.....	24
TRANSVERSE AND LONGITUDINAL CRACKING.....	25
PLASTIC SHRINKAGE CRACKING.....	28
SURFACE FIBERS.....	28
STRUCTURAL DESIGN.....	31
CONCEPT.....	31
FAILURE CRITERIA.....	31
PERFORMANCE CRITERIA.....	33
STRESS CALCULATION.....	34
OVERLAY DESIGN.....	39
CONDITIONS AND RECOMMENDATIONS.....	42
REFERENCES.....	44

LIST OF FIGURES

<u>Figure No.</u>		<u>Page</u>
1	Typical corner crack in steel fiber-reinforced concrete.....	4
2	Deteriorated corner crack in steel fiber-reinforced concrete.....	4
3	Multiple cracks in steel fiber-reinforced concrete.....	5
4	Tight midslab longitudinal crack in trafficked area.....	5
5	Tight midslab longitudinal crack in untrafficked area.....	6
6	Crack pattern development, Tampa airfield pavement.....	8
7	Edge cracking, Tampa airport pavements.....	10
8	Development of additional cracking between older sealed cracks, Tampa airport pavement.....	10
9	Development of crack and spalling, Tampa airport pavement.....	11
10	Shrinkage required to cause 1/4-in. curl.....	21
11	Cracking tensile stress for slabs subject to volume change with discontinuous base shear restraint.....	26
12	Tensile stress developed for 25-ft-wide placement lanes at several airports.....	27
13	Cracking at doweled longitudinal joint, Denver Airport.....	28
14	Examples of variable final finish of fiber- reinforced concrete.....	30
15	Average reduction in flexural strength for cracked beams after 1.5 years exposure to seawater.....	32
16	Steel fiber-reinforced concrete performance criteria using percent standard thickness.....	34
17	Resilient modulus data for lean clay used in MESL construction.....	37
18	Steel fiber-reinforced concrete performance criteria using Westergaard based design factor.....	38
19	Steel fiber-reinforced concrete performance criteria using elastic layer based design factor.....	39

LIST OF TABLES

<u>Table</u>		<u>Page</u>
1	Typical Steel Fiber Characteristics Used in Airfield Pavements.....	3
2	PCI Rating of Reno Fiber-Reinforced Overlay.....	13
3	Selected Characteristics of Inspected Pavements.....	17
4	Interim Suggested Slab Dimensions and Maximum Joint Spacing for Steel Fiber-Reinforced Concrete.....	24
5	Field Tests of Fiber-Reinforced Concrete Pavements.....	33
6	Steel Fiber-Reinforced Concrete Test Items.....	36
7	Performance Calculation for Steel Fiber-Reinforced Concrete.....	38
8	Comparison of Overlay Design Equations and Item 3 Performance.....	42

## INTRODUCTION

### BACKGROUND

In 1974 the Federal Aviation Administration (FAA) and US Army Engineer Waterways Experiment Station (WES) published a technical report providing background, proposed design procedures, and recommended construction practices for steel fiber-reinforced concrete in airport pavements. In August 1979 the Department of the Army issued a new airfield rigid pavement design manual,<sup>10</sup> that allowed the use of steel fiber-reinforced concrete and provided design and construction procedures that drew heavily on Parker's work.<sup>16</sup>

Although the Department of the Army was one of the first Federal agencies to publish design and construction procedures for steel fiber-reinforced concrete pavements, its actual experience with the material in pavement construction is limited. This experience consists of several accelerated aircraft traffic test sections,<sup>6,5</sup> an experimental test road at WES,<sup>16</sup> a tank parking hardstand at Fort Hood,<sup>22</sup> and an accelerated tank traffic test section.<sup>11</sup>

At the time of Parker's work in 1974 the only actual use of steel fiber-reinforced concrete airfield pavement had been a small trial overlay at Tampa, Florida.<sup>15</sup> Since then several steel fiber-reinforced concrete pavements have been used at commercial airports and Navy airfields. At some of these there have been reports of unsatisfactory performance of steel fiber-reinforced pavements. The Federal Aviation Administration was therefore concerned about the cause of these problems and how they related to their previously sponsored research.

### SCOPE

The study reported herein reviews the problems and performance of selected steel fiber-reinforced concrete pavements at civilian airports and military airfields. Its purpose is to determine what revisions of the current design and construction procedures are appropriate and what areas require further research.

## FIELD SURVEY

### INTRODUCTION

Steel fiber-reinforced concrete pavement has been used at two Naval Air Stations and at least seven commercial airfields. These are Norfolk Naval Air Station, Norfolk, Virginia; Fallon Naval Air Station, Fallon, Nevada; Newark International Airport, Newark, New Jersey; John F. Kennedy International Airport, New York, New York; Stapleton International Airport, Denver, Colorado; Tampa International Airport, Tampa, Florida; McCarran International Airport, Las Vegas, Nevada; Cannon International Airport, Reno, Nevada; and Salt Lake City International Airport, Salt Lake city, Utah. These pavements, with the exception of Newark and John F. Kennedy, were visually inspected as part of this study. Pavement performance was discussed with airfield and airport operators, though no testing or detailed evaluation was done.

The purpose of the field survey was to determine what problems existed and what immediate revisions to TM 5-824-3 are necessary, and to identify problem areas that might require further work.

### NORFOLK NAVAL AIR STATION, VIRGINIA

Steel fiber-reinforced concrete has been used in three areas at Norfolk Naval Air Station: a bonded overlay on the main runway above a roadway tunnel, a small light-aircraft parking apron, and a 55-acre\* aircraft parking apron. The runway overlay was not available for inspection for this survey. The aircraft parking apron is at present used only by light aircraft for the local flying club, but it was originally designed for much heavier military cargo aircraft. This apron appears to be in good condition as it is subjected to insignificant loading.

Most of the inspection time was spent at the 55-acre aircraft parking apron. The existing apron had been overlaid with steel fiber-reinforced concrete in five separate construction projects beginning in 1977 and extending into 1982. The concrete mix used in the overlay consisted of 600 lb of type I portland cement and 250 lb of fly ash per cubic yard reinforced with Fibercon steel fibers (four projects) or 85 lb of Bekaert Steel's Dramix ZP 50/.50 fiber (1980 project). Typical characteristics of steel fibers used in airfield paving are shown in Table 1. Maximum nominal size aggregate was 3/8 in. and water reducing and air-entraining admixtures were used. The concrete was cured by covering it with polyethylene for 7 days.

The original pavement at the site was a 7-in.-thick concrete slab built on fill in 1943 and overlaid with 2 in. of asphaltic concrete in 1966. The steel fiber-reinforced concrete overlays were placed directly on the asphaltic concrete. This overlay is typically 5 in. thick with longitudinal butt construction joints and saw cut transverse construction joints. Slabs are 25 by 25 ft. There are a few 7-in.-thick steel fiber-reinforced concrete slabs adjacent to the aircraft hangers that supplement the parking apron.

---

\* A table of factors for converting non-SI units of measurement to SI (metric) units is presented on page ii.

Table 1  
Typical Steel Fiber Characteristics Used in Airfield Pavements

Manufacturer	Length in.	Cross Section or Diameter in.	* $\frac{l}{d}$	Comments
Bekaert Dramix ZP 50/.50	2.0	0.02	100	Deformed end
Fibercon	1.0	0.01 × 0.22	19	Rectangular cross section
Atlantic Wire	2.5	0.025	100	--

\* Ratio of length to diameter, calculated for rectangular cross section by using equivalent diameter that gives same cross sectional area.

Slab curling is a problem throughout the fiber-reinforced concrete overlay and is sometimes clearly visible. Curling of pavement slabs occurs when the top and the bottom of the slab are subject to differential volume changes which results in a warped slab. Potential causes of this curling will be discussed in detail later in the report. The upward warped corners are vulnerable to overstressing due to the lack of support at the corners. Under traffic this results in corner cracking. In trafficked areas corner cracks are common, and sometimes all four corners at joint intersections have cracks. Typically, these consist of a crack 1 to 3 ft from the corner, such as that shown in Figure 1. The cracks are generally tight, without spalling. Occasionally, corner cracks have deteriorated, and in extreme cases, the corner has sheared off the slab and can be depressed as much as 1/2 in. below the upward warped slab. A typical deteriorated corner crack is shown in Figure 2, and a corner with two cracks is shown in Figure 3.

The upward warped slab corners leave a void between the slab and underlying asphaltic concrete, and infiltrating water is frequently trapped under slab corners. In extreme cases, it is possible for a man standing on a slab corner to pump water up through the joints. Surface stains from pumping are evident.

There were occasional tight longitudinal cracks such as those seen in Figures 4 and 5. These existed in both trafficked and untrafficked portions of the apron. Some delayed joint sawing on one project also resulted in a few transverse contraction cracks.

For the portions of this project that were constructed in 1977, often only about every third saw cut joint actually cracked and left effective slabs 25 ft wide and 75 ft long. Excessive movement at the joint for slabs of this length can cause joint sealant failure. In later construction, the depth of the saw cut was increased from 1/4 of the slab thickness to 1/3 of the slab thickness which seemed to allow the saw cut joints to crack properly.

#### FALLON NAVAL AIR STATION, NEVADA

Steel fiber-reinforced concrete was used at this site to overlay an aircraft parking apron. The overlay was constructed in two projects in 1980

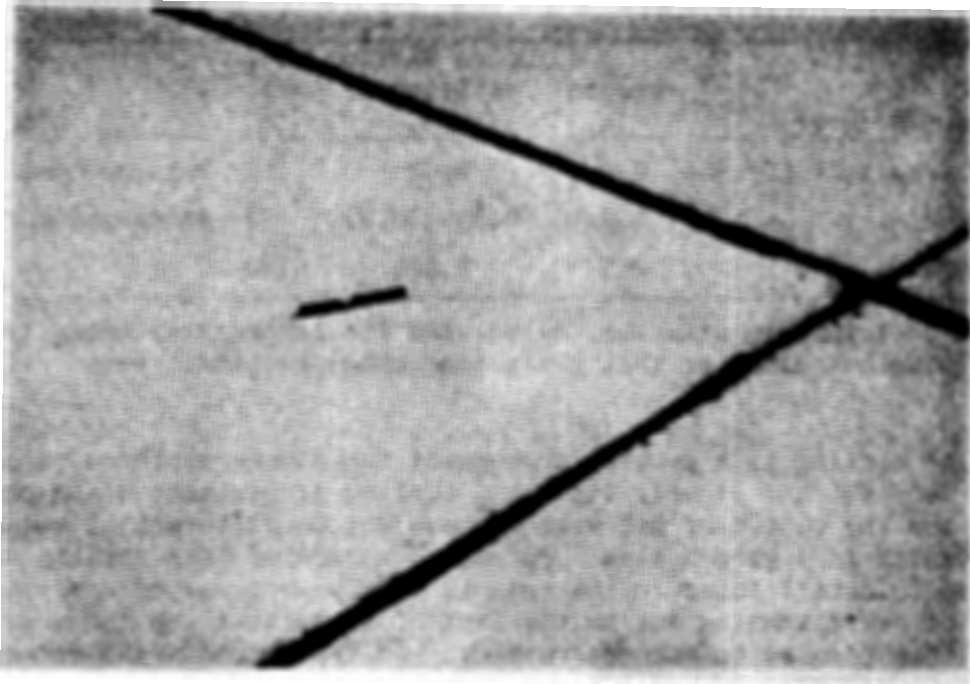


Figure 1. Typical corner crack in steel fiber-reinforced concrete

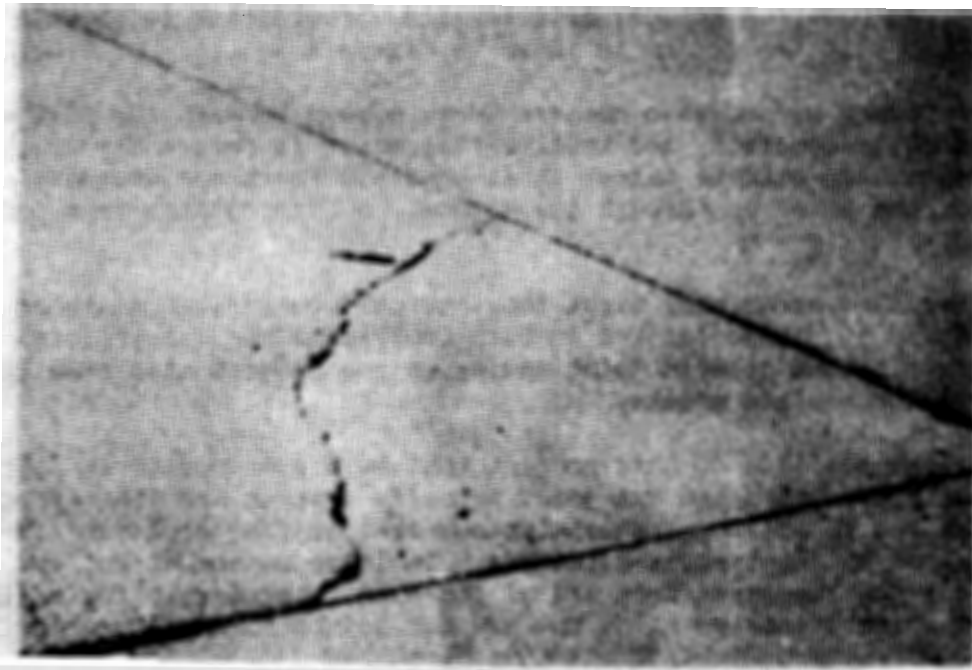


Figure 2. Deteriorated corner crack in steel fiber-reinforced concrete

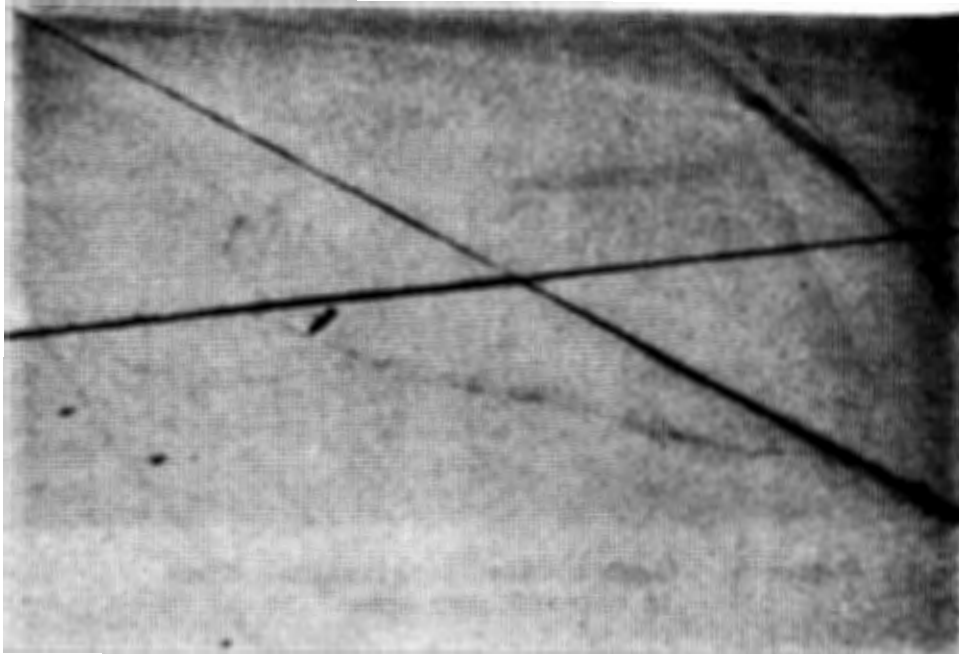


Figure 3. Multiple cracks in steel fiber-reinforced concrete



Figure 4. Tight midslab longitudinal crack in trafficked area

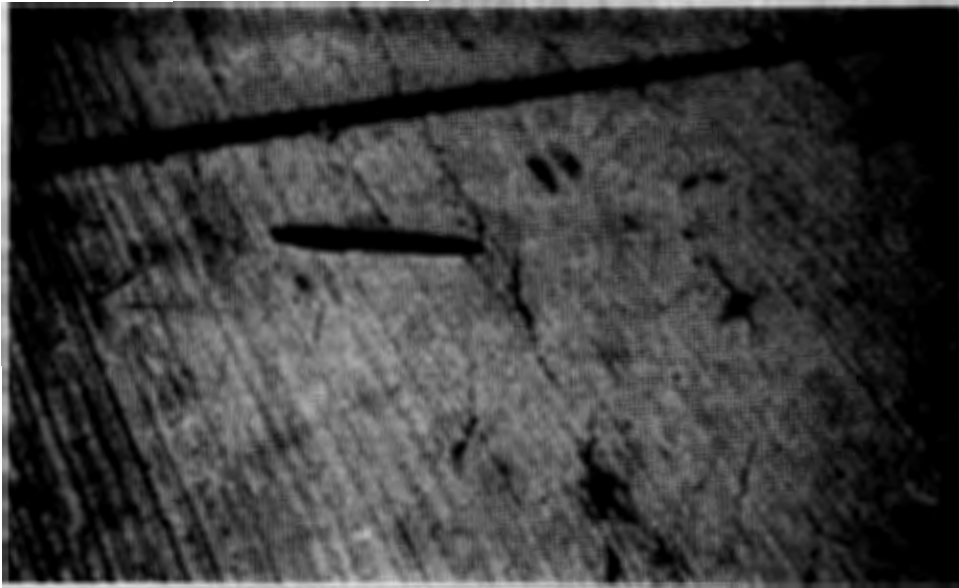


Figure 5. Tight midslab longitudinal crack  
in untrafficked area

and 1981. The 1980 project consisted of a 40,000-sq-yd by 5-in.-thick steel fiber-reinforced concrete overlay on a 2-in.-thick asphaltic concrete overlay of a portland cement concrete pavement. The 1981 project was an 88,000-sq-yd overlay of 5 in. over the same older pavement.

The 1980 concrete contained 788 lb of type II modified portland cement per cubic yard and 82 lb of Bekaert ZP 50/.50 steel fiber per cubic yard. The maximum nominal size aggregate was 3/4 in.; the water cement ratio was 0.43, and water reducing and air entraining admixtures were used. The 1981 concrete was similar with 766 lb/yd<sup>3</sup> of type II portland cement, 81 lb/yd<sup>3</sup> of Bekaert ZP 50/.50 steel fiber, a water cement ratio of 0.45, but no water reducing admixture was used. Both projects were slipformed in 25-ft-wide lanes with longitudinal butt construction joints. Transverse construction joints were all saw cut at 40-ft intervals. White pigmented membrane curing compound was used on both projects.

Slab curling exists in the pavement of each project, and aircraft traffic has resulted in corner cracking. However, damage is more extensive in the older project, and there are also a few tight longitudinal cracks similar to those in Figures 4 and 5. Some of the transverse saw cuts did not crack, so there were some effective slabs of 80 to 120 ft in the first project.

A serious concern has developed at Fallon due to loose fibers on the pavement surface. After 2 to 3 years, steel fibers continue to come loose on the surface and periodic sweeping with a magnet is still required to pickup loose fibers. These loose fibers are viewed as a potential safety hazard and a potential foreign object damage (FOD) source for high-performance military jet aircraft. Loose and protruding fibers on the pavement surface are an obvious nuisance to maintenance personnel who must work on aircraft parked on the pavement. A-7 aircraft operate regularly from these surfaces, and other

aircraft use them periodically. During the time these pavements have been in service, actual engineer damage due to fibers have been reported; however, the Navy has decided to stop using steel fiber-reinforced concrete pavement until this potential problem is evaluated.

#### TAMPA INTERNATIONAL AIRPORT

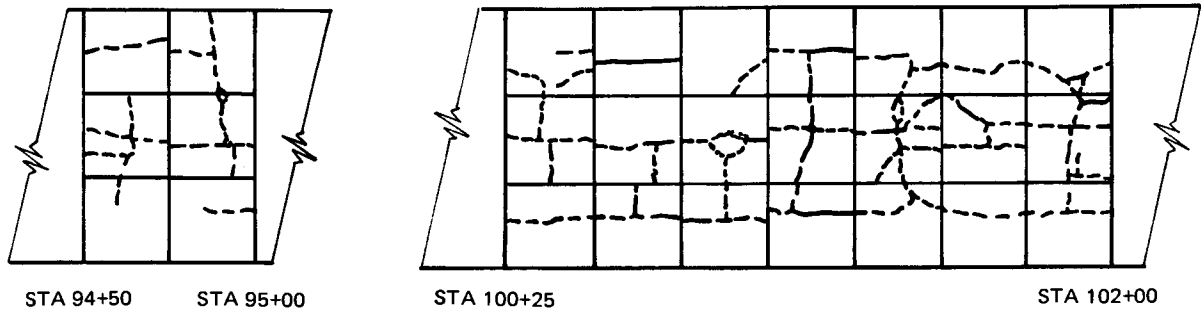
A 4- and a 6-in. steel fiber-reinforced, partially bonded overlay was placed on a taxiway at Tampa International Airport in 1972. The construction of this overlay has been reported in detail by Parker.<sup>15</sup> The original base pavement was badly cracked 12-in.-thick portland cement concrete over a 3-in.-thick limerock base over the native sand subgrade. This relatively small project was undertaken to see if conventional concrete batching and placing equipment could handle fiber-reinforced concrete on a full sized field job.

The concrete mix design used for the steel fiber-reinforced concrete overlay was 517 lb/yd<sup>3</sup> of type I portland cement, 225 lb/yd<sup>3</sup> of fly ash, and 200 lb/yd<sup>3</sup> of Fibercon fibers. Maximum nominal size aggregate was 3/4 in.; water/cement ratio was 0.37, and retarding and air entraining admixtures were used. The field beam samples had an average flexural strength of 1,007 psi at 90 days. The 4-in. overlay was slipformed in two 25-ft-wide by 50-ft-long lanes. The 6-in. overlay was slipformed in three 25-ft-wide by 175-ft-long lanes. All longitudinal construction joints were butt joints, and no transverse contraction joints were used. A white pigmented membrane compound was used for curing. Surface preparation of the base pavement prior to overlay consisted only of removing loose material and extruded joint sealant and wetting the surface. Both overlays are classified as partially bonded overlays.

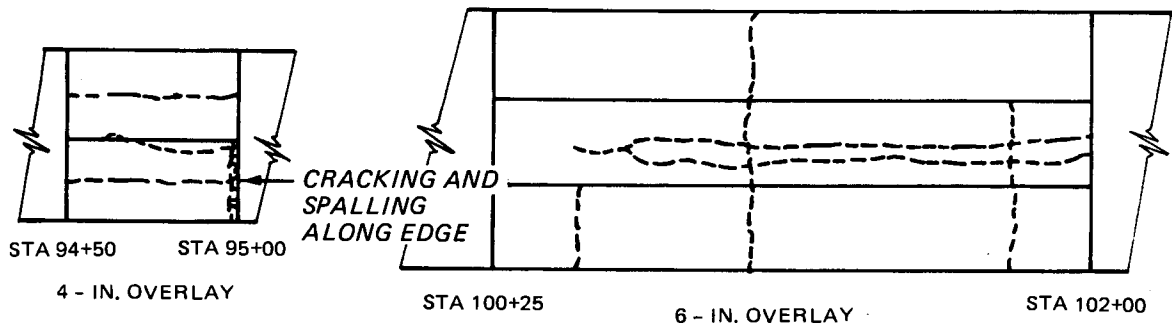
Figure 6 shows the original crack patterns in the base pavement and the progression of cracking in the overlay project through the next 12 years. Within 6 months cracks in the base pavement began to reflect through both overlays. Also, by this time, the lower transverse joint edge at sta 95+00 of the 4-in. overlay had begun failing badly with intersecting cracks and spalling. Reflective cracking continued in both the 4- and 6-in. overlays. Load-related intersecting cracks and spalling developed in the 4-in. overlay as early as 6 months and became extensive by 9-1/3 years. The 6-in. overlay has some load-related cracking at sta 102 at 9-1/3 years and this deteriorated into faulting, additional cracking, and spalling at 12-1/3 years. Load-related cracking appeared to begin at the transverse construction joints at the project ends where edge loading and high stresses would be expected. Figure 7 shows the extent of cracking at the edge of the fiber-reinforced pavement, and Figure 8 shows the development of additional cracking between older sealed cracks. Figure 9 shows the development of spalling along some cracks. Corner cracking such as that seen in Figures 1 through 3 was not observed in Tampa.

#### McCARRAN INTERNATIONAL AIRPORT

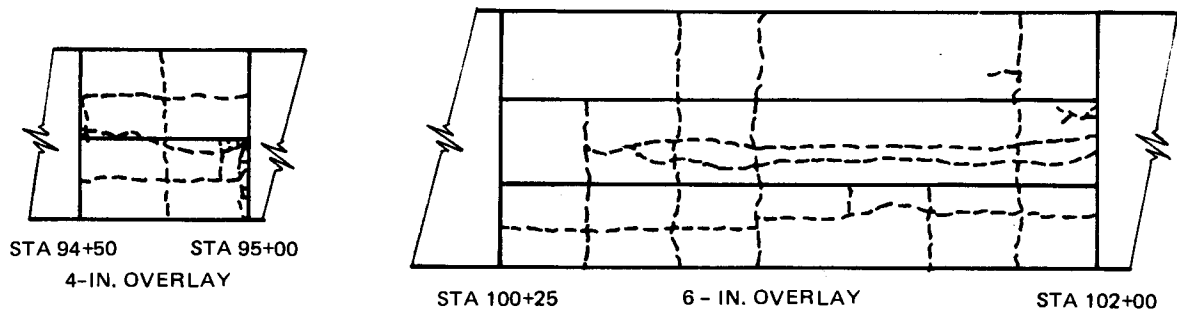
Two steel fiber-reinforced concrete pavements have been placed at McCarran Airport at Las Vegas, Nevada. In 1976, a 63,000-sq-yd by 6-in.-thick fiber-reinforced concrete overlay was placed over a transient aircraft apron pavement of 2 in. of asphaltic concrete and 18 in. of base course. In 1979 a 74,000-sq-yd by 8-in.-thick fiber-reinforced concrete terminal apron pavement was placed over 2 in. of asphalt concrete and 12 in. of aggregate base course.



a. Joint and crack pattern in base pavement, 2/72

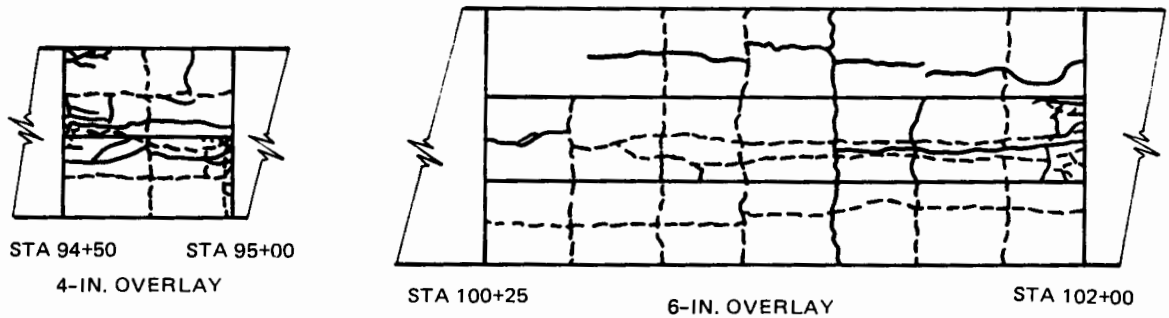


b. Crack pattern in overlays--6 months, 8/72

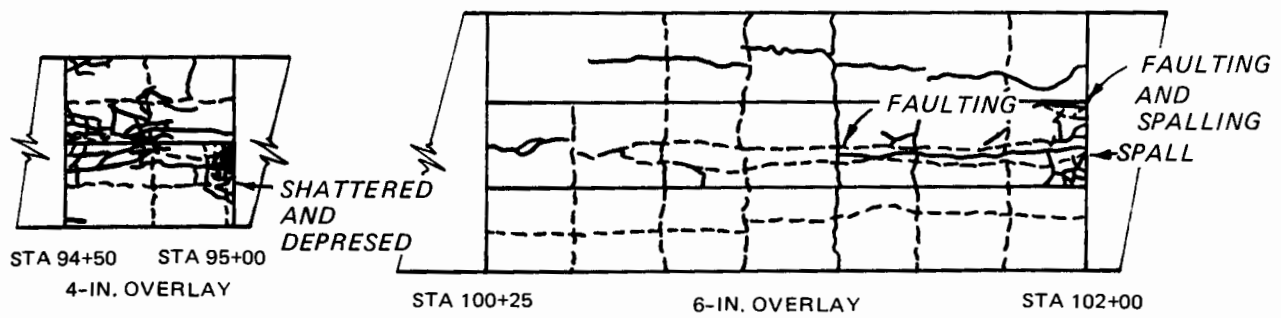


c. Crack pattern in overlays--28 days, 6/74

Figure 6. Crack pattern development, Tampa airfield pavement (Continued)



d. Crack pattern in overlays--112 months (9-1/3 years), 6/81



e. Additional damage observed--148 months (12-1/3 years), 6/84

Figure 6. (Concluded)



Figure 7. Edge cracking, Tampa airport pavements

Figure 8. Development of additional cracking between older sealed cracks, Tampa airport pavement



a. Cracking with development of spalling



b. Cracking with more severe spalling

Figure 9. Development of crack and spalling, Tampa airport pavement

Materials used in the 1976 transient aircraft apron were 600 lb of type V sulfate resistant portland cement, 250 lb of class F fly ash, and 160 lb Fibercon steel fiber per cubic yard of concrete. Maximum nominal aggregate size was 3/8 in.; water-cement ratio was 0.42, and water reducing and air entraining admixtures were used. Materials used in the 1979 terminal apron were 650 lb of type II modified portland cement and 252 lb of fly ash with 85 lb of Bekaert ZP 50/.50 steel fibers per cubic yard of concrete. Maximum nominal aggregate size was 3/8 in.; water-cement ratio was 0.38, and again, water reducing and air-entraining admixtures were applied. Longitudinal construction butt joints were used at 25-ft spacings, and transverse construction joints were saw cut at 50-ft spacings on both projects. A white pigmented membrane compound was used for curing.

Corner cracking is a common distress in both projects. Some tight longitudinal cracking exists in both projects, but is more prevalent in the 1976 transient aircraft apron. There has been a problem with recurring joint sealant failure since some of the saw cut transverse joints failed to crack through the slab. This resulted in effective slab lengths of 100 or 150 ft, and the excessive temperature movements of the slabs caused joint seal failures.

#### CANNON AIRPORT

In 1975 a 54,000-sq-yd, 4-in.-thick steel fiber-reinforced concrete overlay was bonded to a badly cracked and spalled concrete terminal apron at Cannon Airport at Reno, Nevada. In 1980 a 33,000-sq-yd, 8-in.-thick taxiway was built of steel fiber-reinforced concrete, but it was not available for inspection because of heavy aircraft traffic. Only the 1975 bonded terminal apron overlay will be discussed here.

Materials for the fiber-reinforced concrete overlay were 658 lb/yd<sup>3</sup> of portland cement and 216 lb/yd<sup>3</sup> of fly ash with 200 lb/yd<sup>3</sup> of Fibercon steel fiber. The nominal maximum size aggregate was 3/8 in.; the water-cement ratio was 0.36, and water reducing and air entraining admixtures were used. The overlay matched the original pavement's 20- by 25-ft-joint pattern. The steel fiber-reinforced overlay used a bonding medium such as grout and extensive surface preparation to obtain a bond between the overlay and base pavement. This termed a fully bonded overlay but details on construction methods and quality are not available at this time.

The overlay is largely unbonded now, and water trapped beneath the slabs results in pumping. There is considerable cracking of the overlay. Table 2 shows the detailed results of a 1983 pavement condition index (PCI) rating of the overlay. Corner breaks are a common distress, but there is a significant amount of other types of distress that contribute to the overall PCI rating of 55 (fair). There is no detailed information on the cracking pattern of the original pavement, so it is not possible to determine how much of the longitudinal and transverse cracking in the overlay is reflective cracking from the underlying pavement. Despite the amount of cracking that exists, there is little spalling or deterioration of the cracks.

Table 2  
PCI Rating of Reno Fiber-Reinforced Overlay

<u>Distress Type</u>	<u>Severity</u>	<u>Density, %</u>	<u>Deduct Value</u>
Corner break	Low	12.28	9.5
	Medium	3.27	5.4
	High	0.81	2.0
	Total	16.36	
Longitudinal, transverse, diagonal crack	Low	6.78	6.3
	Medium	7.83	16.2
	High	1.52	6.0
	Total	16.13	
Joint seal damage	Low	9.23	2.0
	Medium	77.07	7.0
	High	13.56	12.0
	Total	99.86	
Small patching	Low	0.58	0.0
Pumping	--	--	7.25
Shattered slab	Low	1.52	3.8
	Medium	0.81	4.0
	Total	2.33	
Shrinkage cracks	--	--	67.83
Joint spalling	Low	1.87	1.2
	Medium	0.11	0.1
	High	0.11	0.3
	Total	2.09	
Corner spalling	Low	1.75	0.6
	Medium	1.52	1.2
	Total	3.27	

Note: Overall PCI of 55 (fair) is based on PCI of 23 random samples. PCI standard deviation between samples was 22.6. PCI conducted by Education Research Engineering Services, Inc., Champaign, Ill., using procedures of FAA-RD-80-55.<sup>20</sup>

## SALT LAKE CITY INTERNATIONAL AIRPORT

Steel fiber-reinforced concrete was used at the Salt Lake City airport for rehabilitation of an aircraft parking apron. In 1980 a 4,000-sq-yd, 8-in.-thick steel fiber-reinforced concrete pavement was placed on a 8-in.-thick cement stabilized base. This work continued in 1981 with a 31,000-sq-yd placement. This placement consisted of 7- and 8-in.-thick steel fiber-reinforced concrete over varying sections of 12 in. of existing portland cement concrete, 5-1/2 to 8 in. of old asphaltic concrete, and 6 in. of lean concrete over varying thicknesses of gravel. A 1-in.-thick leveling and bond breaking course of asphaltic concrete was used between the underlying materials and the fiber-reinforced concrete.

The 1980 placement contained 583 lb/yd<sup>3</sup> of type II portland cement, 203 lb/yd<sup>3</sup> of fly ash, and 83 lb/yd<sup>3</sup> of Bekaert ZP 50/.50 steel fibers. The maximum nominal aggregate size was 3/8 in.: water reducing and air entraining admixtures were used, and the water-cement ratio was 0.42. The 1981 placement concrete contained 620 lb/yd<sup>3</sup> of type II portland cement, 215 lb/yd<sup>3</sup> of fly ash, and 85 lb/yd<sup>3</sup> of Bekaert ZP 50/.50 steel fiber. Aggregates were similar, as well as the water reducing and air entraining admixtures which were also used; the water-cement ratio was 0.38. Concrete was placed in formed 50-ft-wide lanes. A longitudinal saw cut contraction joint was located at the mid-point of each lane, and transverse saw cut contraction joints were placed at 35-ft spacings. All longitudinal and transverse joints were doweled. White pigmented membrane curing compound was used on both projects.

Extensive transverse plastic shrinkage cracking exists throughout the apron. Much of the concrete placement was done at night to avoid unfavorable temperature and drying conditions that existed during construction, but, apparently, the procedures used were not adequate to prevent the cracking. Slab curling and corner breaks have not been a problem at Salt Lake City, and only one corner crack was observed in the areas inspected for this project. The saw cut longitudinal joints did not crack, and only every third or fourth saw cut transverse joint cracked. The effective slab sizes are 50 by 105 or 140 ft which results in large movements at the joints and sealant failures.

## STAPLETON AIRPORT

In 1981 Denver's Stapleton airport used steel fiber-reinforced concrete for an 84,000-sq-yd apron overlay and reconstruction. The fiber-reinforced concrete was placed in 7- and 8-in.-thick sections. The 7-in.-thick pavement was an overlay of a cracked 12-in.-thick reinforced concrete pavement that had an 8-in.-thick crushed aggregate base. The 8-in.-thick fiber-reinforced pavement was used in the reconstructed portions of the project and was placed over a 15-in. cement-treated base that was above a 12-in.-thick lime-treated subgrade layer. Both the overlay and the reconstructed portion of the project used an asphalt-impregnated fabric between the fiber-reinforced concrete and the underlying layer.

The fiber-reinforced concrete was composed of 525 lb/yd<sup>3</sup> of type I portland cement, 250 lb/yd<sup>3</sup> of fly ash, and 83 lb/yd<sup>3</sup> of Bekaert ZP 50/.50 steel fiber. After the start of the project, the concrete mixture was adjusted to provide 575 lb of cement and 210 lb of fly ash per cubic yard. The maximum

nominal aggregate size was 3/4 in.; the water-cement ratio was 0.37, and water reducing and air entraining admixtures were used. Flexural strengths were reported to be 750 psi at 7 days and 1,000 psi at 14 days.

Concrete was placed by slipforming in 25-ft lanes. All longitudinal construction joints were doweled, and transverse contraction joints were saw cut to a depth of 3 in. at 30-ft spacing. A white pigmented membrane compound was used for curing.

Within a week of placement, slab curling was evident to airport personnel. This has resulted in extensive corner cracking throughout the area. Most cracked corners have remained intact, but in heavily trafficked areas some of the corners have been sheared off from the slab. Amount of slab curl is estimated to be 1/4 to 3/8 in., but one extreme of 5/8 in. has been reported.

There is some plastic shrinkage cracking in some of the initial placement of concrete, but this is an isolated distress. Occasional transverse cracking exists in some areas. It is located near and parallel to saw cut joints. There are also some longitudinal cracks close to and parallel to the doweled longitudinal joints. Tight longitudinal cracks are sometimes found near the center of some slabs. This transverse and longitudinal cracking is not common, and these problems are not as severe as the corner cracking. Most saw cut joints reportedly cracked and are functioning properly.

## ANALYSIS OF FIELD PROBLEMS

Review of the field survey of selected steel fiber-reinforced concrete airfield pavements found that several problems existed with the performance of these pavements. Almost universally, slab curling was a problem that commonly resulted in corner breaks when the curled corners were subjected to traffic. Also, saw cut contraction joints sometimes failed to crack which caused excess joint movement at working joints and resulted in joint sealant failures. Other problems that were not common at all sites were transverse and longitudinal cracking, plastic shrinkage cracking, and exposed fibers on the pavement surface. Each of these problems are discussed individually.

### CURLING

Slab curling is a frequent problem in steel fiber-reinforced concrete airfield pavements and is of such concern that Bekaert Steel Corporation sponsored an independent study of curling by Schrader and Lankard.<sup>18</sup> The major functional problem with curling is that it leads to corner breaks when the slab is trafficked. It is widely recognized that some curling occurs with conventional concrete pavements. Nevertheless, curling with accompanying corner breaks under traffic is not nearly so severe in conventional concrete pavements as in steel fiber-reinforced concrete pavements.

Fiber-reinforced concrete pavement curl values reported by Schrader and Lankard<sup>18</sup> range from 1/8 to 5/8 in. These values were measured as the maximum distance from the slab surface to a stringline stretched between the corners of the slab. One obstacle to recognizing slab curl in the field is the normally small magnitude of the curl and the difficulty of measuring it. One of the most reliable indicators of curling is the development of corner cracking under traffic, but this is only an indicator when the pavement is exposed to reasonably heavy loads. For instance, the heavily loaded Denver apron developed corner cracks very rapidly. However, the light aircraft parking apron at Norfolk would not be expected to develop corner cracking under the light loads of the local flying club airplanes even if curl did exist in the slab. Of the pavements inspected and listed in Table 3, only Salt Lake City and Tampa failed to have significant corner cracking problems when exposed to traffic. An examination of Table 3 shows no consistent characteristics of these pavements that might explain the variation in corner cracking.

Curling in fiber-reinforced pavement typically appears early. In the extreme case of Denver it was visually noticeable within a week. The only mechanism that will explain curling is a differential volume change between the top and the bottom of the slab with the top shortening more than the bottom. Furthermore, this curl is a permanent characteristic of the pavement which does not disappear with time, environmental change, etc. Volume changes in concrete can occur due to setting and hydration of cement, drying shrinkage, temperature differentials between the slab faces, and carbonation. These potential sources of volume change that lead to differential shrinkage need to be examined in detail to determine those that cause the permanent early age curl in steel fiber-reinforced concrete pavements.

Table 3  
Selected Characteristics of Inspected Pavements

Project	Date Constructed	Cement/Fly Ash lb/yd <sup>3</sup>	W/C* Ratio	Type Cement	Fiber lb/yd <sup>3</sup>	Fiber Reinforcement Type	Estimated** Aggregate Vol. %	Cure Time	Underlying Layer	Bond to Underlying Layer	Slab Size Thickness ft x ft x ft	Severity of Corner Cracking
Norfolk apron	1977 to 1982	600/200	-- --	I	160 85	Fibercon Bekaert	--	7 days	Asphalt	Unbonded	25 x 25 x 5	Severe
Denver apron	1981	575/210	0.37	II	83	Bekaert	62	7 to 14 days	Fabric	Unbonded	25 x 30 x 7 or 8	Severe
Las Vegas apron	1976	600/250	0.42	V	160	Fibercon	56	Several months 1 year	Asphalt	Unbonded	25 x 50 x 6	Moderate
	1979	650/252	0.38	II	85	Bekaert	60				25 x 50 x 8	
Fallon apron	1980	788/0	0.43	II	82	Bekaert	60	--	Asphalt	Unbonded	25 x 40 x 5	Moderate
	1981	766/0			81	Bekaert	58					
Reno apron	1975	658/216	0.36	--	200	Fibercon	51	--	Concrete	Fully bonded	25 x 20 x 4	Moderate
Salt Lake City apron	1980	583/203	0.42	II	83	Fibercon	56	2 to 3 weeks	Asphalt	Unbonded	25 x 30 x 7 or 8	Minor
	1981	620/215	0.38	--	85	Fibercon	57					
Tampa taxiway	1972	517/225	0.37	I	225	Fibercon	--	6 days	Concrete	Partial bond	25 x 75 x 4 25 x 175 x 6	None

\* Calculated as weight of water ÷ (weight of cement + weight of fly ash).

\*\* Calculated as Aggregate Volume × weight of Aggregate per cubic yard of concrete ÷ (specific gravity aggregate × unit weight of water × 27). Aggregate specific gravity assumed to be 2.65.

## SHRINKAGE

Carbonation shrinkage of the surface is a long-term effect that fails to explain the early curl observed in the inspected fiber-reinforced pavements. Plastic or capillary shrinkage occurs while the concrete is still plastic and also is not a likely contributor to slab curl. Thermal gradients in the slab can be developed by environmental conditions or by heat developed during hydration of the portland cement. The environmental gradient is developed by heating and cooling the slab's exposed surface and results in volume change in the surface. This may add to the curling problem in fiber-reinforced concrete, but it is a reversible process that varies at different times of day and with different seasons. Temperature-induced curling is discussed at length in standard pavement texts such as Yoder and Witczak,<sup>24</sup> but it is not a mechanism that is compatible with the permanent, early-age curl observed in fiber-reinforced concrete pavement slabs.

Schrader and Lankard<sup>16</sup> in their analysis of curling in fiber-reinforced airfield slabs concluded that:

The second phenomenon (i.e. high temperature in the lower part of the slab during early ages because of heat of hydration of the cement) has been neglected by design and construction personnel but it is unquestionably the culprit causing early age curl that takes a permanent set and later results in corner cracks or high-edge stresses.

This explanation has several problems. First, the thinness of the slabs raises the question whether or not the high temperature gradient postulated by Schrader and Lankard could develop in 4- to 8-in.-thick slabs. Further, although the mixes in question have high contents of cementitious materials with potentially high hydration exotherms, Table 3 shows that, with only one exception, fly ash was used to partially replace portland cement and that type II or V portland cement was commonly used. Fly ash can be conservatively estimated to contribute 15 to 35 percent of the early heat of hydration of an equivalent amount of portland cement,<sup>1</sup> and types II and V portland cement typically have a lower heat of hydration than type I. In the pavements examined for this study, design and construction personnel had generally used materials that would minimize the heat of hydration problem, and the thin slabs should provide ample surface area relative to their volume to allow reasonable dissipation of heat. Table 3 fails to show any relation between the severity of corner cracking and cement content, type of cementitious materials, or slab thickness. Such a relationship would be expected if the premise that heat of hydration caused slab curling were correct.

If a large temperature gradient from cement hydration developed in the slabs so that the bottom of the slab was at a higher temperature than the surface, the lower portion of the slab would increase in volume relative to the surface and result in an upward curled slab. However, the process is reversible, and as the high heats from hydration dissipate, the lower portion of the slab will decrease in volume. A permanent set will occur only if the concrete's coefficient of thermal expansion decreases between the time of the early buildup of the heat of hydration and its later cool down within a few days. Some data reported by Neville<sup>14</sup> show that the coefficient of thermal

expansion generally increases between 28 and 90 days, but it is a complex function of curing conditions and the concrete's constituents. Schrader and Lankard's<sup>18</sup> contention that the thermal gradient from hydration is the cause of permanent curl would require that the coefficient of thermal expansion decrease with age which is the opposite of the trend of the data reported by Neville.<sup>14</sup> The explanation of permanent early-age slab curl as a function of heat hydration buildup in the slab is not supported by the field performance of the pavements listed in Table 3, nor is the mechanism necessary to develop permanent curl from hydration temperatures supported by available data.

Drying shrinkage occurs when water is withdrawn from concrete. When the upper portions of a paving slab dry out and the lower portions do not (a very common field condition), a shrinkage gradient develops across the slab that can cause curling. As water is withdrawn from the slab surface, surface volume decreases while the volume at the bottom of the slab remains unchanged. This differential volume change of shrinkage can result in curling. Typical laboratory values of drying shrinkage may vary from approximately  $300 \times 10^{-6}$  to  $1,000 \times 10^{-6}$  percent. There is a great deal of variation due to many factors including environment, test procedures, aggregate, water content, and mixture proportions.

Drying shrinkage does not begin until effective curing is over, and water can be lost from the concrete. All of the inspected projects in Table 3, with the exception of Norfolk, used membrane curing. Until curing is discontinued or until the pavement is opened to traffic, thereby wearing away the membrane, drying shrinkage should not occur. Neville<sup>14</sup> suggests that 14 to 34 percent of the 20-year value of drying shrinkage is reached within 2 weeks of the end of curing, 40 to 80 percent within 3 months, and 66 to 85 percent within 1 year. The rapid occurrence of curling almost before curing is complete, as within a week at Denver, suggests that drying shrinkage is an inadequate explanation for the rapid curling observed in fiber-reinforced concrete pavements. Also, Salt Lake City had extensive plastic shrinkage cracking which suggests extensive loss of surface moisture. This is the condition favorable to drying shrinkage curling, but curling is not a major problem at this airport. At later times in the pavement life drying shrinkage may add to the magnitude of curl, but it is not a satisfactory explanation alone for the permanent early-age curl.

Under normal pavement construction conditions, portland cement decreases in volume as it reacts with water, and the amount of volume decrease is proportional to the degree of hydration. A gross volume decrease of approximately 7 percent of the portland cement and water volume has been observed.<sup>4</sup> Increasing cement content and temperature tend to increase this volume change.<sup>14</sup> Other factors affecting this change seem to be composition of cement, its fineness, quantity of mixing water, mixture proportions, and curing conditions.<sup>21</sup>

The autogenous shrinkage due to hydration would not cause warping in an unrestrained member, but the friction between the bottom of the pavement slab and the underlying material would resist any volume change that affected the bottom of the slab. The top of the slab is unrestrained, however, and the upper portion of the slab will try to undergo unrestrained shrinkage. At

the same time the bottom portion can undergo a smaller shrinkage due to the frictional resistance. This variation in shrinkage would be a mechanism to cause slab warping. All of the surfaces between the fiber-reinforced concrete and underlying layers in Table 3 could develop significant frictional resistance. The fabric at the Denver airport was impregnated with asphalt to provide a surface that was bonded to the underlying layers and would probably provide frictional resistance.

It appears that the most significant autogenous volume changes occur within 60 to 90 days of placement of the concrete.<sup>21</sup> This fact, in conjunction with the existence of a reasonable curling mechanism described above, seems to offer a promising explanation for the early-age curl observed in fiber-reinforced concrete airfield slabs. The major drawback to this explanation is that autogenous shrinkage is small and usually ignored, except in mass concrete. Neville<sup>14</sup> suggests that typical values for autogenous shrinkage vary from about  $40 \times 10^{-6}$  percent at one month to  $100 \times 10^{-6}$  percent at 5 years. This is only on the order of 5 to 30 percent of the potential volume changes given earlier for drying shrinkage.

#### SHRINKAGE CALCULATION

Some method is now needed to assess the magnitude of shrinkage that will cause curl in typical fiber-reinforced slabs. ACI 209R-82<sup>2</sup> offers the following method for calculating shrinkage deflection for uniform beams:

$$a_{sh} = \epsilon_w \phi_{sh} l^2 \quad (1)$$

where

- $a_{sh}$  = deflection due to shrinkage
- $\epsilon_w$  = a deflection coefficient that depends on boundary conditions
- $\phi_{sh}$  = curvature due to shrinkage warping
- $l$  = length

A fixed end cantilever beam can be used to approximate the boundary conditions of a slab on grade by treating one half of the slab as a cantilever beam with fixed end at the middle of the slab. The boundary conditions at the fixed end of the beam and the middle of the slab, both deflection ( $w$ ) and slope ( $dw/dx$ ), equal to zero. For this case  $\epsilon_w$  in the above equation is 1/2, and  $l$  is 1/2 of the slab length.

Miller<sup>12</sup> developed an expression for the shrinkage curvature ( $\phi$ ) as

$$\phi_{sh} = \frac{\epsilon_{sh} - \epsilon_s}{d} \quad (2)$$

where

- $\epsilon_{sh}$  = free shrinkage per unit of length of the concrete assumed to be equal to the shrinkage at extreme fiber of the beams
- $\epsilon_s$  = strain in the steel due to shrinkage
- $d$  = effective depth of the beam

For the unreinforced concrete pavement slab this expression becomes

$$\phi_{sh} = \frac{\Delta\epsilon_{sh}}{h} \quad (3)$$

where

$\Delta\epsilon_{sh}$  = differential shrinkage between top and bottom fibers of the beam  
 $h$  = thickness of slab

The original equation for the deflection due to shrinkage can be re-written to solve for the required differential shrinkage to cause a given deflection as

$$\Delta\epsilon_{sh} = \frac{a_{sh} h}{\epsilon_w \ell^2} \quad (4)$$

or for a cantilever beam and length of slab  $L = 2\ell$  as

$$\Delta\epsilon_{sh} = \frac{8a_{sh} h}{L^2} \quad (5)$$

Figure 10 shows the minimum differential shrinkage that would cause a 1/4-in. curl as calculated by the above equation for different slab thicknesses and lengths. Using the maximum slab lengths and the thicknesses shown in Table 3, Tampa would curl for differential shrinkages of  $10 \times 10^{-6}$  or more,

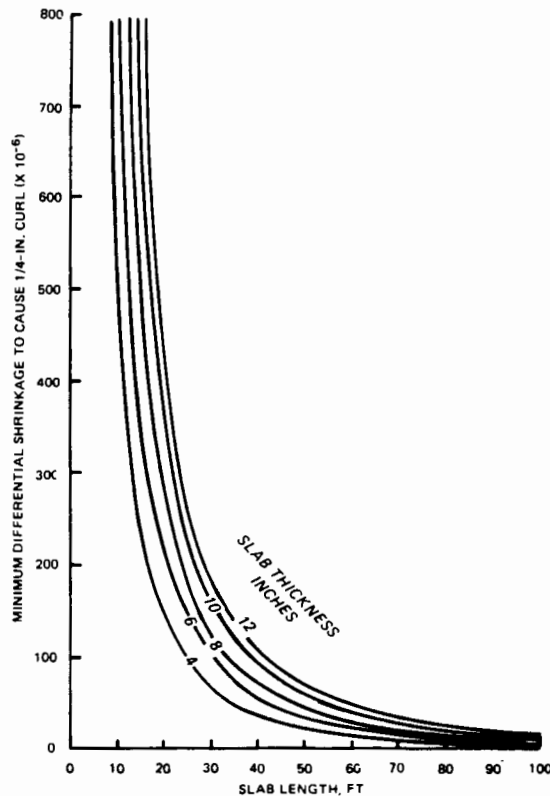


Figure 10. Shrinkage required to cause 1/4-in. curl

Las Vegas for  $35$  and  $45 \times 10^6$  or more, and all others for differential shrinkages of  $110$  to  $122 \times 10^6$  or more.

These are generally slightly higher than the values of autogenous shrinkage quoted earlier from Neville.<sup>14</sup> However, several points need to be considered. First, the calculated shrinkages are the amount of differential shrinkage between top and bottom of the slab and, consequently, depend on the slab's resistance to moving or bonding to the underlying layer. Experience with continuously reinforced and prestressed concrete pavements indicates substantial frictional resistance between a concrete slab and underlying layers. The 1/4-in. curl used in the calculations for Figure 10 is not an unusual observed value in the field; however, it is measured at the corner of the slab. The idealization of considering a unit width of the slab to be equivalent to a cantilever beam for the calculations is approximately correct near the center of the slab. Near the corners, contributions to curl come from both the longitudinal and transverse directions, and the idealization begins to break down. Consequently, curl at the slab corner is always the maximum curl in the slab, and the 1/4-in. magnitude of curl for the model used for calculation in Figure 10 represent a very severe condition. If a lower magnitude of curl is selected, such as 1/8 in., the required differential shrinkage is reduced directly, in this case by half. From these considerations it appears that typical autogenous shrinkage magnitudes could be enough to cause curling in fiber-reinforced pavement slabs.

#### VOLUME CHANGE MECHANISMS

Volume change characteristics have not been studied in depth for fiber-reinforced concrete and are an area for further study. However, autogenous shrinkage in fiber-reinforced concrete can be expected to be higher than in conventional paving concrete. The amount of this volume change is a direct function of the content of cementitious material, and fiber-reinforced concrete pavement have a higher cementitious material content than conventional paving concrete. Also volume change is resisted by aggregate, and mixtures containing large-sized aggregate and a large volume of aggregate have smaller overall concrete volume change than those with small sizes and volumes of aggregate. The fiber-reinforced concrete pavements inspected for this study had maximum aggregate sizes of 3/8 and 3/4 in. and typically had aggregate volumes of 51 to 62 percent of the total. These are all smaller than conventional paving concrete. The large cementitious material content of fiber-reinforced concrete in conjunction with typically smaller sized aggregate and lower aggregate volumes suggests that fiber-reinforced concrete would have larger autogenous shrinkage than that normally encountered in conventional paving concrete. However, volume change effects and the influence of fibers on this have not been studied adequately and are an area requiring further research.

#### APPROACHES TO CURLING PROBLEM

Autogenous Shrinkage. Autogenous shrinkage resisted by frictional forces between the bottom of the slab and the underlying layers offers the most promising explanation of the curling problem in fiber-reinforced concrete pavements. This explanation agrees with the early age at which curl is observed, and autogenous shrinkage is large enough to cause curl for the slab lengths and thicknesses used in fiber-reinforced airfield pavements. This is further supported when consideration is given to the facts that Figure 10

represents a severe state of curl and the fiber-reinforced concrete used in these projects had characteristics that could be expected to increase autogenous shrinkage compared to conventional paving concrete. The other potential explanations of high heat of hydration and drying shrinkage are less promising as discussed earlier, although they may contribute to the magnitude of the problem at different times.

Of the inspected pavements, Tampa and Salt Lake City had no or very limited curling and corner cracking. Tampa was a partially bonded overlay; so there was more resistance (i.e. the bonds between overlay and base pavement) to curling than would occur with an unbonded overlay. Reflective cracking from the joints and extensive cracking of the base pavement also helped to reduce the effective slab size and to reduce curling. However, if the bond between overlay and base pavement avoided curling in Tampa, it should have done even better for the stronger fully bonded overlay in Reno. This was not the case as shown in Tables 2 and 3. Very little information is available on construction methods, quality of construction, condition of the base pavement, or when curl and corner cracking developed at Reno. Consequently, the curling with resulting corner cracks at Reno may be due to problems such as poor bonding grout between overlay and base which eventually weakened and failed under longer term cyclic warping stresses caused by the large environmental temperature changes possible in Reno. This is a very different phenomena from the permanent early-age curl discussed previously. It seems reasonable to expect partial and fully bonded overlays to resist curling better than unbonded overlays.

Salt Lake City had a very limited amount of curling and corner cracking but was an unbonded overlay. Slab sizes and thicknesses and mixture proportioning are not sufficiently different from other projects listed in Table 3 to explain the difference in performance. Salt Lake City did have the most extensive problem with widespread plastic shrinkage cracks caused by excessive moisture loss at an early age. These cracks do not extend through the slab. The plastic shrinkage cracks may provide sufficient relief to allow the surface shrinkage to occur without restraint. The effect of shrinkage would be to open up the surface cracks rather than warp the slab upwards.

There has not been enough research work done on defining the volume change characteristics of steel fiber-reinforced concrete. Both laboratory and field work are needed to investigate this more thoroughly. In the interim, prevention of curl in fiber-reinforced concrete pavements is going to require limiting the slab dimensions to levels that avoid this problem. The present design manual's<sup>10</sup> allowable joint spacing of 50 ft for 4- to 6-in.-thick fiber-reinforced pavements and 100 ft for greater than 6-in.-thick fiber-reinforced pavements should not be used. Until more research is completed, it is recommended that slab dimensions for fiber-reinforced concrete be limited to those shown in Table 4. These are based on allowable dimensions presently in use by the Corps of Engineers for plain paving concrete except that the minimum allowable thickness has been reduced to 4 in. Also shown in Table 4 are the minimum differential shrinkage levels required to cause 1/4- to 1/8-in. curls calculated as described earlier. These values are approximately three times greater than those presented earlier for the pavements listed in Table 3.

Table 4  
Interim Suggested Slab Dimensions and Maximum Joint  
 Spacing for Steel Fiber-Reinforced Concrete

Slab Thickness in.	Suggested Maximum Joint Spacing ft	Differential Shrinkage To Cause 1/4-in. Curl ( $\times 10^{-6}$ )	Differential Shrinkage To Cause 1/8-in. Curl ( $\times 10^{-6}$ )
4-6	12.5	356-533	712-1,066
6-9	15.0	370-556	740-1,112
9-12	20.0	313-417	626-834
>12	25.0	>267	>553

Friction-Reducing Layer. Another approach to preventing curl in fiber-reinforced concrete pavements is to reduce the friction that develops between the fiber-reinforced slab and the underlying layer so that volume change in the lower portion of the slab is not restrained. This can be accomplished by using a friction-reducing layer between the pavement slab and underlying layer. A layer consisting of a thin (1/4- to 1/2-in.) layer of sand covered with two layers of polyethylene has been used under prestressed pavements to reduce the frictional forces that must be overcome in post-tensioning. A similar layer may be successful in reducing early curl in fiber-reinforced pavements; however, these slabs may then become vulnerable to later drying shrinkage and temperature induced curling. Reports by Wu<sup>23</sup> and Schrader and Lankard<sup>18</sup> indicate curling and corner cracks were less severe at some fiber-reinforced concrete pavements at JFK airport in New York than at some of the other airports. The pavements at JFK airport did use a polyethylene sheet as a bond breaker between the fiber-reinforced overlay and base pavement. This may have helped reduce frictional restraint on the bottom of the slab. More research is needed to determine if this is an effective approach to avoiding curling and to determine reasonable slab sizes for this construction.

#### JOINT PERFORMANCE

Several of the inspected projects had cracking problems with saw cut contraction joints due to the high tensile strength provided by the steel fibers. This strength was sufficient to prevent cracking under all the contraction joint saw cuts, and only every second or third joint cracked properly. This resulted in large effective slab sizes with large movements at the functioning joints that did crack. These large movements result in rapid failure of the joint sealants and are a continual maintenance problem.

This problem was largely solved during construction by increasing the depth of the saw cut from 1/4 of the slab thickness to 1/3 or 1/2 of the thickness. The design manual<sup>10</sup> should direct that saw cut contraction joints for steel fiber-reinforced concrete pavements be made to a minimum 1/3 of the slab thickness for slabs 6 in. or thicker or to 2 in. for slabs less than 6 in. thick.

## TRANSVERSE AND LONGITUDINAL CRACKING

The most extensive transverse and longitudinal cracking was encountered at Tampa and Reno airports. These overlays were both bonded to some degree and were thin (4 to 6 in.) as well. Underlying pavements in both cases were cracked and in poor condition. A large amount of the cracking that developed was undoubtedly reflective cracking, but, as discussed earlier, some of the later progressive cracking at Tampa was load related.

Bonded (as at Reno) and partially bonded (as at Tampa) conventional concrete overlays are not considered satisfactory for overlaying badly cracked and deteriorated base pavements. This is because the underlying cracks will reflect through the overlay in a short time. Tampa and Reno show that the higher tensile strength of fiber-reinforced concrete is not enough to prevent the progressive development of reflective cracks. Bonded overlays should only be used for surface restoration of pavements that are essentially in good structural condition. Partially bonded overlays should be restricted to use on base pavements that may have some limited structural cracking, but the cracking remains generally tight without spalls and unfaulted. If the base pavement is badly cracked and deteriorated, an unbonded overlay should be used. In both bonded and partially bonded overlays the overlay joints should match the base pavement joints.

Isolated incidents of transverse cracking were probably due to late sawing. These were not a common form of distress, and normal construction procedures are adequate to prevent this.

At the Norfolk, Denver, and Las Vegas airfields longitudinal cracks existed in the approximate center of the slab and ran through multiple slabs. Typical cracking is shown in Figures 4 and 5. This type of cracking is probably due to the same restraint against volume change that caused the problem of slab curling. ACI 207.2R-73<sup>1</sup> provides a method of examining the tensile stress necessary to cause cracking in a slab with discontinuous shear restraint on the bottom and subject to a volume change. A crack will begin at the approximate center of the slab when a parabolic tensile stress distribution develops through the slab depth with the stress at the base of the slab equal to the tensile strength of the concrete. The cracking moment associated with this stress distribution is

$$M_{cr} = \frac{f'_t B H^2}{10} \quad (6)$$

where

$M_{cr}$  = cracking moment associated with parabolic tensile stress distribution

$f'_t$  = tensile strength of concrete and maximum stress at base of slab

B = width of cross section

H = thickness of slab

This cracking is resisted by an external balancing moment due to the weight of concrete and can be expressed as

$$M_r = 0.075 W B H L^2 \quad (7)$$

where

$M_r$  = restraining moment due to weight of concrete resisting curl

$W$  = unit weight of slab

$L$  = length of slab

The tensile stress that will initiate cracking can be found by setting  $M_{cr}$  equal to  $M_r$  and solving for  $f'_t$ . Taking  $W$  as 145 lb/ft<sup>3</sup> and expressing  $L$  in feet,  $H$  in inches, and  $f'_t$  in lb/in.<sup>2</sup> this becomes

$$f'_t = 9.0625 \frac{L^2}{H^2} \quad (8)$$

Figure 11 shows the tensile stress calculated from the above equation that will develop cracking for slabs of various thicknesses and lengths. The midslab longitudinal cracking seemed to be most prevalent at Norfolk, Las Vegas, and Denver, and the tensile stresses for these locations are shown in Figure 12. These stresses range from 705 to 1,150 psi. Steel fiber-reinforced concrete commonly develops 900- to 1,100-psi flexural strength for paving mixes which would appear to be adequate to resist the tensile stresses encountered in Denver and Las Vegas. However, these stresses develop as volume change occurs, so the development of cracking requires that the volume change must produce these critical cracking stresses before the concrete develops adequate strength to resist them.

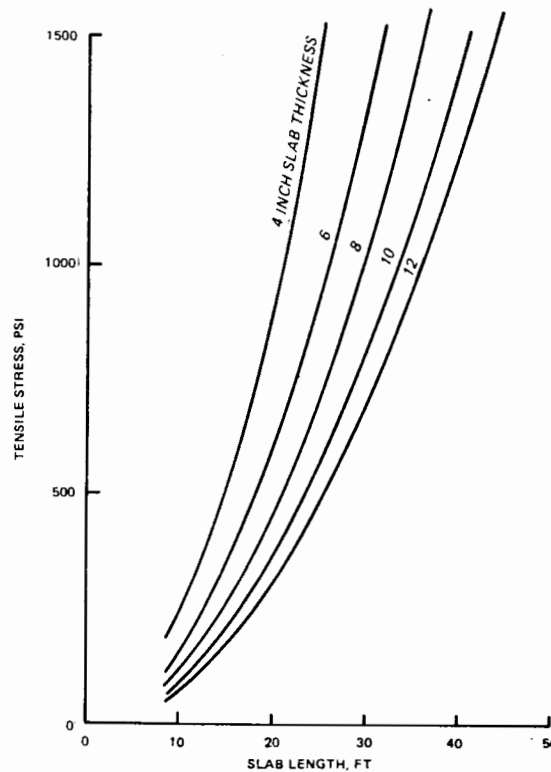


Figure 11. Cracking tensile stress for slabs subject to volume change with discontinuous base shear restraint

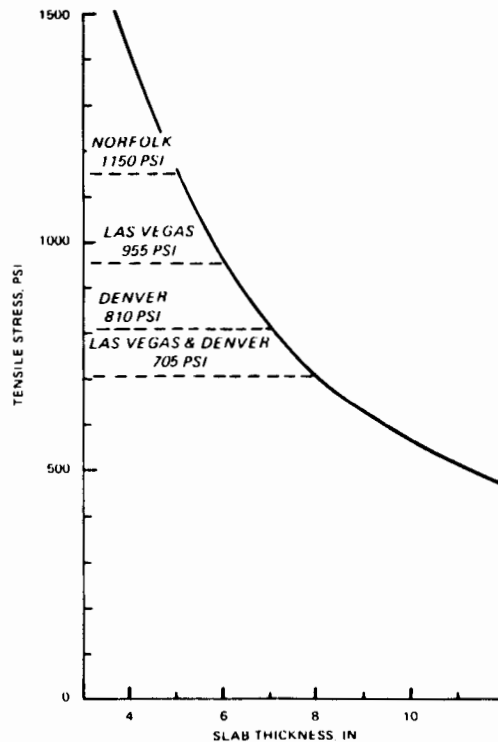


Figure 12. Tensile stress developed for 25-ft-wide placement lanes at several airports

This type of cracking appears to be due to the same volume change and large, thin slabs that caused the problems with slab curling. Use of the recommended slab dimensions shown in Table 4 will maintain the cracking tensile stress in Figure 11 between 340 and 480 psi which is considerably below that found in Figure 12.

The Denver airport developed some cracks approximately over the ends of the dowel bars, resulting in long longitudinal cracks that run parallel to the doweled longitudinal joints. This type of cracking was most noticeable along the doweled longitudinal joint that separated the existing old conventional concrete pavement from the new steel fiber-reinforced concrete. There were a few locations, however, where it developed alongside the doweled longitudinal joints between fiber-reinforced concrete placement lanes.

This cracking adjacent to doweled longitudinal joints at Denver is probably due to the upward curl of the fiber-reinforced concrete slabs. As the fiber-reinforced concrete slab shown in Figure 13 tries to curl upward, it is restrained by the dowels in the adjacent uncurled conventional concrete. This curl is occurring at an early age when the fiber-reinforced concrete is still gaining strength, and a crack forms at the end of the dowel bars to allow the remainder of the slab to curl.

Several mechanisms may occur to help avoid this kind of cracking parallel to a doweled longitudinal construction joint between lanes of fiber-reinforced concrete and to explain its relative infrequency at Denver.

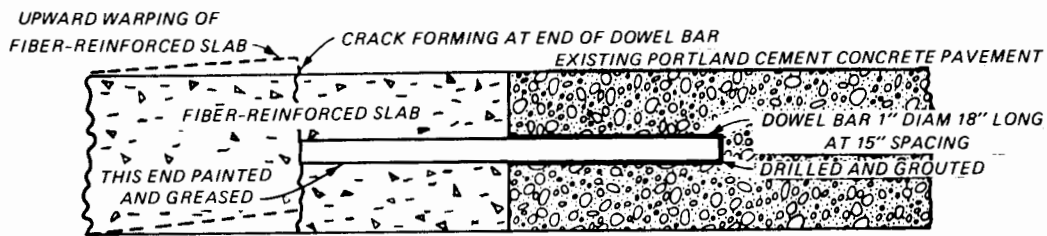


Figure 13. Cracking at doweled longitudinal joint, Denver Airport

Concrete placement usually proceeds by skipping lanes. Dowels are then inserted in holes drilled in the slab edges, and finally concrete is placed in the fill-in lanes. The slab lanes which are first placed and drilled for dowels may have already curled by the time the fill-in lanes are placed. The passage of the equipment placing and finishing the fill-in lanes may deflect the upward curled adjacent slabs downward. After passage of the concrete placement equipment, these slab edges will curl up again and lift the fill-in slab edges or deform the freshly placed concrete sufficiently to allow later upward movement of the dowel bars when the newly placed slab cures. The newly placed concrete of both lanes may also allow sufficient deformation of the concrete around the dowel bars because of low bearing strength at early ages to tolerate some curling. Therefore, curling in adjacent slabs can usually be tolerated without cracks forming over the bar ends.

The problem of longitudinal cracking over the dowel bar ends will be avoided by preventing curling in the slab. Adoption of the maximum slab sizes in Table 3 should largely accomplish this.

#### PLASTIC SHRINKAGE CRACKING

Salt Lake City and Reno had extensive shrinkage cracks. These cracks are believed to be due to excessive rapid loss of water from the surface, although placement conditions and construction procedures are not well enough known to try to identify the specific cause. There is no indication that fiber-reinforced concrete pavement is more susceptible to shrinkage cracking than normal concrete with similar cement, aggregate, and water content. Good construction and curing practices must be followed for all types of concrete to avoid excessive water loss. This is particularly true when construction must be done in hot, dry climates.

#### SURFACE FIBERS

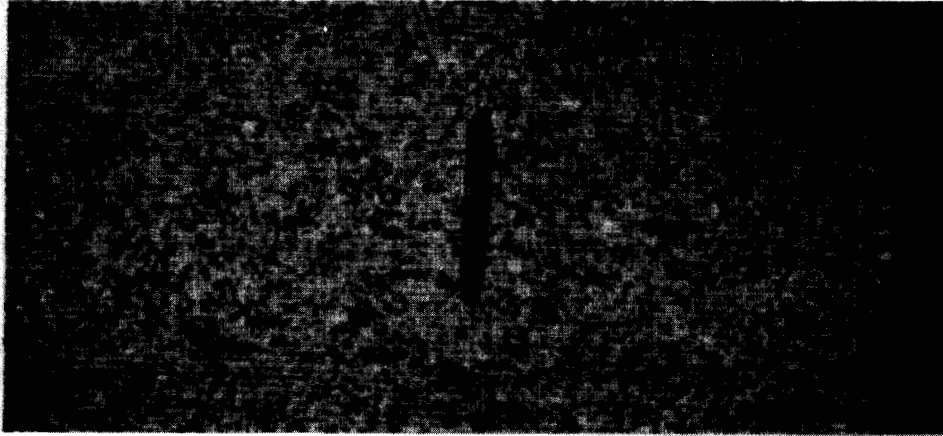
The Navy has expressed concern that loose fibers existing on the pavement surface are a potential threat to the jet engines of military aircraft. There is no evidence to show that any aircraft engine has ever been damaged by fibers. Military A-7 aircraft and commercial B-737 aircraft have operated extensively on steel fiber-reinforced concrete pavements without mishap, and both of these aircraft have low engine air intakes. The greatest potential for ingesting debris in an aircraft engine occurs when a preceding aircraft kicks or blows the debris into the air, and it is encountered by a following aircraft. Even though no data exists to support the contention that the fibers are a hazard to jet engines, it must be studied and positively resolved

one way or the other before the user can be expected to accept the pavement with confidence.

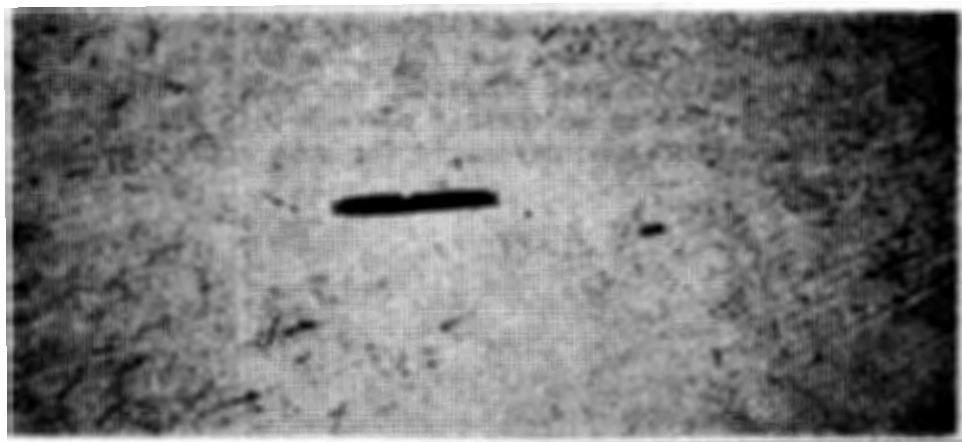
Final finish of fiber-reinforced concrete varies considerably. Examples of the variable finish on the surface can be seen in Figures 1, 2, 3, 8, and 14. Some success in obtaining a finish with minimal exposed fibers has been reported at Fallon Naval Air Station by the use of a "rollerbug." Engineering personnel at Fallon believe that it is feasible to specify and obtain no more than 18 exposed fibers per square yard of pavement surface using the "rollerbug."

Finishing techniques that use a "rollerbug" or jitterbug" that essentially depress fibers and aggregates into the concrete must be used carefully to avoid bringing an excess of paste to the surface. This paste may make the pavement vulnerable to abrasion, freezing and thawing damage, and scaling.

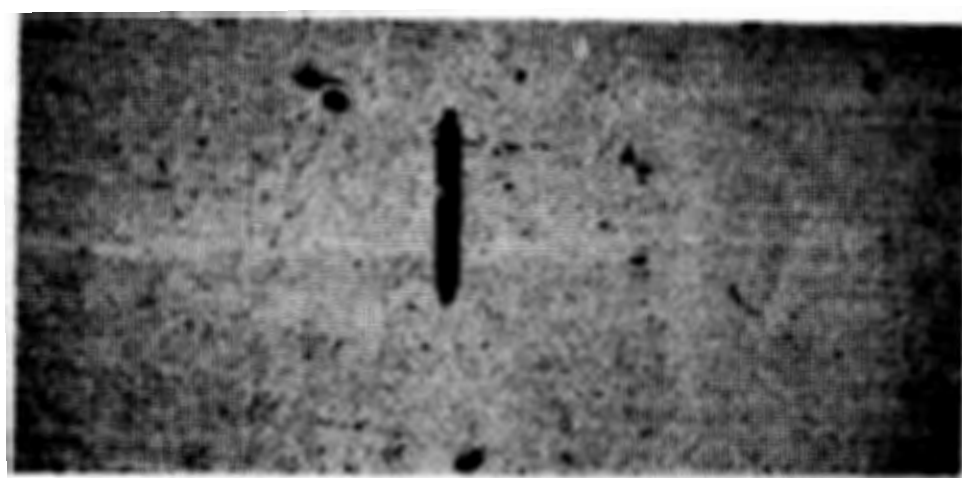
An improved method to consistently provide a finished surface free of loose and protruding fibers must be developed. Loose fibers are perceived as a hazard to certain aircraft. Protruding fibers are a nuisance to maintenance personnel who must work on the pavement surface. The quality of surface finishing has varied considerably on past projects, and until a method is developed that consistently provides an acceptable surface this will be detrimental to the use of steel fiber-reinforced pavements for some applications.



a. Rough texture with excessive exposed fibers



b. Fairly smooth surface with fewer exposed fibers



c. Smooth texture with minimal exposed fibers

Figure. 14. Examples of variable final finish of fiber-reinforced concrete

## STRUCTURAL DESIGN

### CONCEPT

As stated previously, Parker<sup>16</sup> published the first design procedure for steel fiber-reinforced concrete pavement for airfields, and it was adopted for use by the Corps of Engineers in their latest airfield design manual.<sup>10</sup> This design procedure has two major requirements. First, the calculated stresses in the fiber-reinforced concrete must be limited to a level that avoids failure under the design traffic loads and repetitions. Next, the calculated deflections of the overall system must be maintained at levels that have given adequate overall performance in past tests. The first requirement avoids excessive cracking in the slab. The second requirement avoids excessive densification or shear failures in the underlying layers below the pavement slab.

This design procedure produces much thinner pavements for fiber-reinforced concrete than would be obtained for plain concrete pavements for the same design loads. This occurs for two reasons. First, steel fiber-reinforced concrete has an appreciably higher flexural strength than conventional concrete. Further, the existence of a crack in steel fiber-reinforced concrete pavement is not indicative of failure as it normally is for plain concrete pavement. This is because steel fibers are still bridging across the crack and provide considerably more load-carrying capacity until the fibers debond or are broken and the crack opens. Parker<sup>16</sup> took advantage of this property by defining failure of steel fiber-reinforced concrete pavement as the opening of a crack to the extent that load transfer across the crack has been reduced and moisture can enter the crack. This results in corrosion of the fibers in the crack. Using this definition of failure for eight accelerated traffic test sections of fiber-reinforced concrete, Parker<sup>16</sup> defined a new fatigue criteria which allowed a steel fiber-reinforced concrete pavement to carry more load applications than a plain concrete pavement for similar ratios of flexural strength to calculated stress.

The combination of higher flexural strength and the changed fatigue criteria results in steel fiber-reinforced concrete pavements that are typically on the order of half to two-thirds the thickness of a conventional plain concrete pavement. Since these pavements are so much thinner than conventional pavements, Parker<sup>16</sup> added the deflection criteria to the design procedure for steel fiber-reinforced concrete pavements in an effort to avoid problems in the underlying layers. Deflection criteria are not usually applied to conventional plain concrete pavements.

### FAILURE CRITERIA

There has been some concern in the past about corrosion of steel fibers. A recent ACI state-of-the-art report<sup>3</sup> on fiber-reinforced concrete summarizes available research on this, and the results clearly indicate that fiber corrosion is limited to the surface fibers, even when exposed to deicing salts and seawater.

There remains some question of how potential corrosion of the fibers bridging across load-induced cracks would affect Parker's<sup>16</sup> failure criteria

for steel fiber-reinforced concrete. Morse and Williamson<sup>13</sup> conducted several tests to examine the effects of corrosion on fiber-reinforced concrete beams. Beams were made up with three different types of steel fibers. Mixture proportions for all beams were 200 lb/yd<sup>3</sup> of steel fiber, 752 lb/yd<sup>3</sup> cement, 1,500 lb/yd<sup>3</sup> sand, 1,000 lb/yd<sup>3</sup> of 3/8-in. pea gravel, and a water cement ratio of 0.50. Uncracked beams and precracked beams with crack widths of "less than 0.25," 1.6, and 3.2 mm were exposed to twice-a-day saltwater immersion at WES's Treat Island, Maine, test facility for 1.5 years. Figure 15 shows the average reduction of the cracked beam's flexural strength compared with the uncracked beams' strength at the end of this testing. The cracked beams showed depths of fiber corrosions at the crack of 1/8, 1, and 2 in. for the 0.25-, 1.6-, and 3.2 mm crack widths, respectively. The uncracked beams had fiber corrosion on the beam surface only.

These results led Morse and Williamson<sup>13</sup> to define a critical crack width to be 0.25 mm. Additional laboratory tests found that 40 applications of a wet-dry saltwater environment to specimens with crack widths greater than this critical value resulted in sufficient corrosion to destroy the ability of these fibers to bridge the crack. At this point 90 percent of the steel fibers bridging the crack contributed little or no benefit to maintaining the specimen's integrity. This work supports Parker's<sup>16</sup> definition of failure for steel fiber-reinforced concrete pavements. Tight hairline cracks 0.25 mm wide or less do not lead to corrosion of fibers bridging the crack and do not represent failure of the pavement. Once the crack opens to a width greater

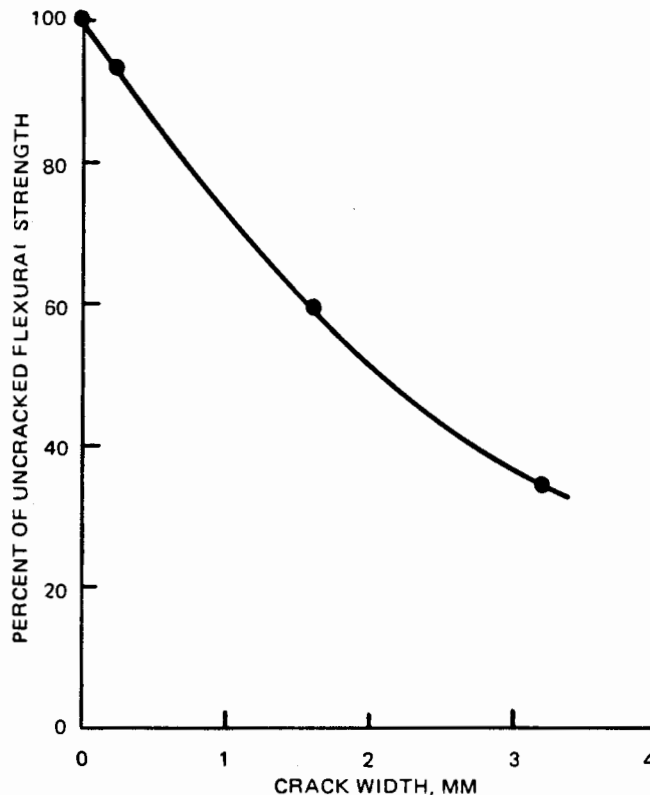


Figure 15. Average reduction in flexural strength for cracked beams after 1.5 years exposure to seawater (after Morse and Williamson<sup>13</sup>)

than this, rapid corrosion of the fibers can occur with a resulting loss of strength and load transfer across the crack.

#### PERFORMANCE CRITERIA

Table 5 lists the available trafficking field tests with steel fiber-reinforced concrete. These are the tests on which Parker<sup>16</sup> based his fatigue or performance criteria relating coverages of traffic to the ratio of flexural strength to calculated stress. The performance of these test items are described in detail by Parker.<sup>16</sup> There were little data available on fiber-reinforced concrete performance under traffic, so Parker<sup>16</sup> drew the performance criteria line for the fiber-reinforced concrete parallel to the conventional Corps of Engineers portland cement concrete criteria and as a conservative interpretation of the available data. This is shown in Figure 16.

A reexamination of the data for the conventional Corps of Engineers concrete pavement criteria revealed that a straight line was better a representation of the relationship than the bilinear line shown in Figure 16.<sup>17</sup> The revised straight line criteria for conventional concrete is shown in Figure 16 along with a revised steel fiber-reinforced concrete criterion that was developed in the same manner used by Parker in 1974.

The conventional standard-thickness method of presenting the Corps of Engineers concrete pavement criteria came into use during the 1950's and has advantages for the manual development of pavement design curves. A standard pavement thickness is defined as that thickness of pavement which, for a specific loading and support condition, gives a design factor of 1.3. A design factor is defined as the flexural strength of the concrete divided by the maximum calculated tensile stress in the pavement. With the advent of computers,

Table 5  
Field Tests of Fiber-Reinforced Concrete Pavements

<u>Test</u>	<u>Item</u>	<u>Load</u>	<u>Coverages to Failure*</u>	<u>Reference</u>
Keyed longitudinal joint study	5	360 kip C-5A gear	350	Grau <sup>6</sup>
		166 kip dual tandem gear	80	
Keyed longitudinal joint study	3	360 kip C-5A gear	2,800	Grau <sup>6</sup>
		166 kip dual tandem gear	950	
Structural layers test section	1	200 kip dual tandem gear	1,000	Burns <sup>5</sup>
		240 kip dual tandem gear		
Structural layers test section	2	200 kip dual tandem gear	500	Burns <sup>5</sup>
		240 kip dual tandem gear	150	

\* Fiber reinforced failure defined to be opening of a crack to sufficient degree to allow moisture.

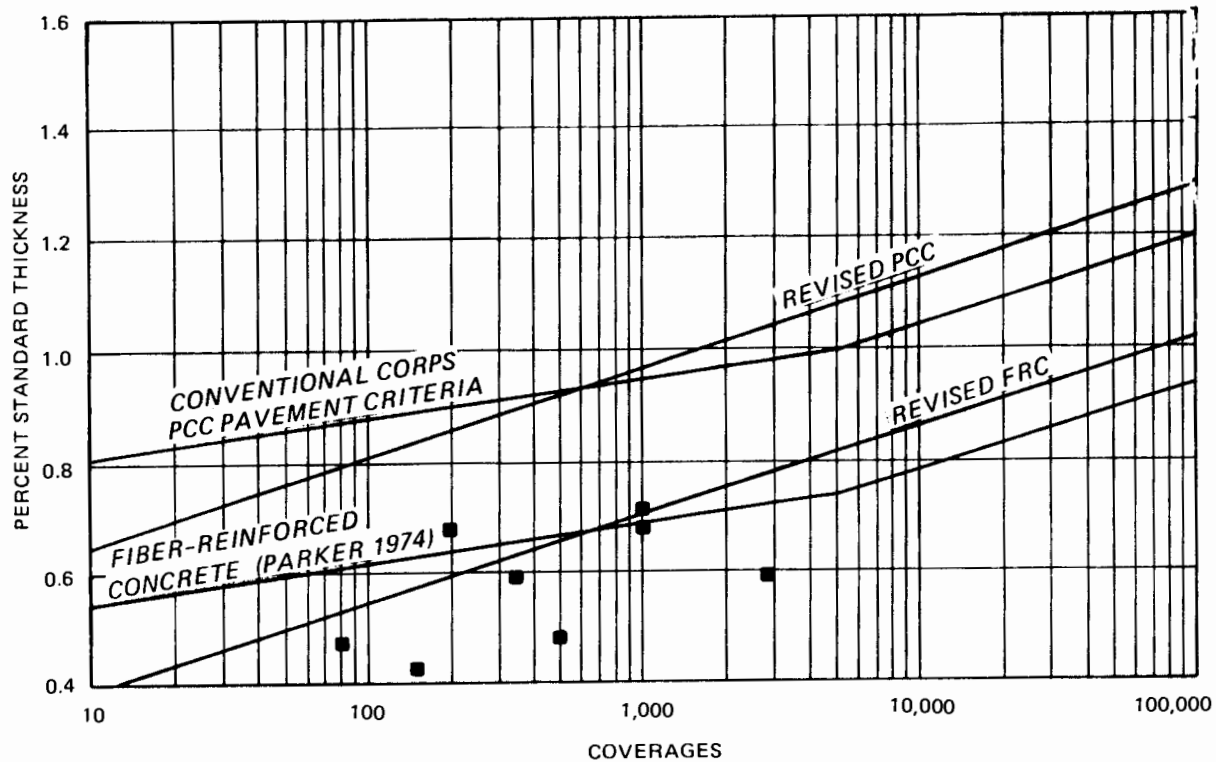


Figure 16. Steel fiber-reinforced concrete performance criteria using percent standard thickness

the time saving advantages of using the percent standard thickness have largely disappeared. The Corps of Engineers concrete pavement performance criteria are now calculated in terms of design factor versus coverages.

The stresses used in the design factor have in the past all been calculated for Corps of Engineers work with the Westergaard edge-loaded model. This model represents the concrete pavement as a slab with the load adjacent to the free edge, the slab infinite in the other three directions, and the slab supported on a bed of springs. Past field tests have generally found that one-fourth of the load applied to the slab edge is carried over to the adjacent slab by means of dowels, keys, aggregate interlock, etc. Consequently, the design factor calculated for the Westergaard model uses the concrete flexural strength divided by three fourths of the Westergaard calculated edge stress.

#### STRESS CALCULATION

The Westergaard model uses the modulus of elasticity and Poisson's ratio to characterize the concrete pavement slab, but all underlying layers are combined and described with a single-value spring constant. This single-value spring constant is a major limitation of the Westergaard model and has led to the use of an elastic layer model to calculate stresses for some problems involving complex layering, stabilized materials, and interpretation of non-destructive test results. The elastic layer model characterizes each layer as continuous, homogeneous, and isotropic and uses modulus of elasticity and

Poisson's ratio to characterize each layer. The slab edge can no longer be modeled because of the assumption of a continuous, homogeneous layer. The design factor for the elastic layer model is calculated as the flexural strength of concrete divided by the elastic layer calculated stress. No reduction is made for load transfer. Of the two models, the Westergaard remains the most widely used.

Because the Westergaard and elastic layer analytical models characterize materials differently and calculate stresses for different conditions, the same performance criteria of design factor versus coverages cannot be used for both models. The Corps of Engineers proposed the following performance criteria to be the best representation of accelerated traffic tests of plain concrete for each of these models:

$$DF_W = 0.50 + 0.25 \log (\text{coverages}) \quad (9)$$

$$DF_{EL} = 0.54 + 0.38 \log (\text{coverages}) \quad (10)$$

where

- $DF_W$  = design factor for the Westergaard model =  $R/\sigma_w$
- $R$  = flexural strength of concrete
- $\sigma_w$  = Westergaard calculated stress
- $DF_{EL}$  = design factor for the elastic layer model =  $R/\sigma_{el}$
- $\sigma_{el}$  = elastic layer calculated stress

The accelerated traffic tests listed in Table 5 can be used to develop performance criteria for steel fiber-reinforced concrete for both the Westergaard and the elastic-layer models. Table 6 shows the details of each of the test items. The keyed longitudinal joint test Item 3 was an overlay and was not included further in this analysis because of the difficulty of adequately modeling the bond conditions between overlays with present techniques. Overlay design will be discussed separately. Table 6 gives material properties for each layer in the test items. The Westergaard model uses only modulus of elasticity (E) and Poisson's ratio ( $\nu$ ) values for the fiber-reinforced concrete surface and represents all the other layers with a single modulus of subgrade reaction (k) value. The elastic-layer model characterizes each layer with a modulus of elasticity and a Poisson's ratio. Figure 17 presents laboratory resilient modulus test data for the lean clay used in the membrane encapsulated soil layer (MESL) in Item 1 of the structural layer test. A modulus value of 20,000 psi was selected as appropriate for the conditions of this item. Table 7 presents the results of the stress calculations for these test items.

Figures 18 and 19 plot the results of the calculations shown in Table 6 with the performance criteria of plain concrete suggested by the author for each model. The elastic layer data show less scatter than the Westergaard data. This is probably due to the preponderance of the test items using

Table 6  
Steel Fiber-Reinforced Concrete Test Items

---

Keyed Longitudinal Joint Test - Item 5	
6-in. fiber-reinforced concrete	E = $5.6 \times 10^6$ psi; $\nu = 0.20$ ; R = 940 psi
4-in. sand filter (SP)	k = 75 pci; E = 7,500 psi; $\nu = 0.40$
36-in. highly plastic clay (CH)	CBR = 4 ; E = 7,500 psi; $\nu = 0.40$
Native lean clay subgrade (CL)	E = 13,500 psi; $\nu = 0.40$
Keyed Longitudinal Joint Test - Item 3	
4.4-in. fiber-reinforced concrete	E = $5.6 \times 10^6$ psi; $\nu = 0.20$ ; R = 1,050 psi
9.5-in. portland cement concrete	E = $6.4 \times 10^6$ psi; $\nu = 0.20$ ; R = 750 psi
4-in. sand filter (SP)	E = 7,500 psi; $\nu = 0.40$ ; k = 100
36-in. highly plastic clay (CH)	E = 7,500 psi; $\nu = 0.40$
Native lean clay subgrade (CL)	E = 13,500 psi; $\nu = 0.40$
Structural Layers Test Section - Item 1	
7-in. fiber-reinforced concrete	E = $5.6 \times 10^6$ psi; $\nu = 0.20$ ; R = 1,000 psi (200 kip load lane) R = 1,200 psi (240 kip load lane)
20-in. MESL	k = 225 pci; E = 20,000 psi; $\nu = 0.3$
24-in. highly plastic clay (CH)	E = 7,500 psi; $\nu = 0.4$
Native lean clay subgrade (CL)	E = 13,500 psi; $\nu = 0.4$

(Continued)

---

Note: E = modulus of elasticity  
 $\nu$  = Poisson's ratio  
R = modulus of rupture  
k = modulus of subgrade reaction  
CBR = California bearing ratio  
SP = poorly graded sand by Unified Soil Classification System  
CL = clay of low plasticity by Unified Soil Classification System  
CH = clay of high plasticity by Unified Soil Classification System

Table 6 (Concluded)

Structural Layers Test Section - Item 2

4-in. fiber-reinforced concrete	$E = 5.6 \times 10^6$ psi; $\nu = 0.20$ ; R = 1,000 psi (200 kip load lane); R = 1,050 psi (240 kip load lane)
17-in. stabilized clayey gravel	$k = 500$ pci; $E = 200,000$ psi; $\nu = 0.20$
29-in. highly plastic clay (CH)	$E = 7,500$ psi; $\nu = 0.40$
native lean clay subgrade (CL)	$E = 13,500$ psi; $\nu = 0.40$

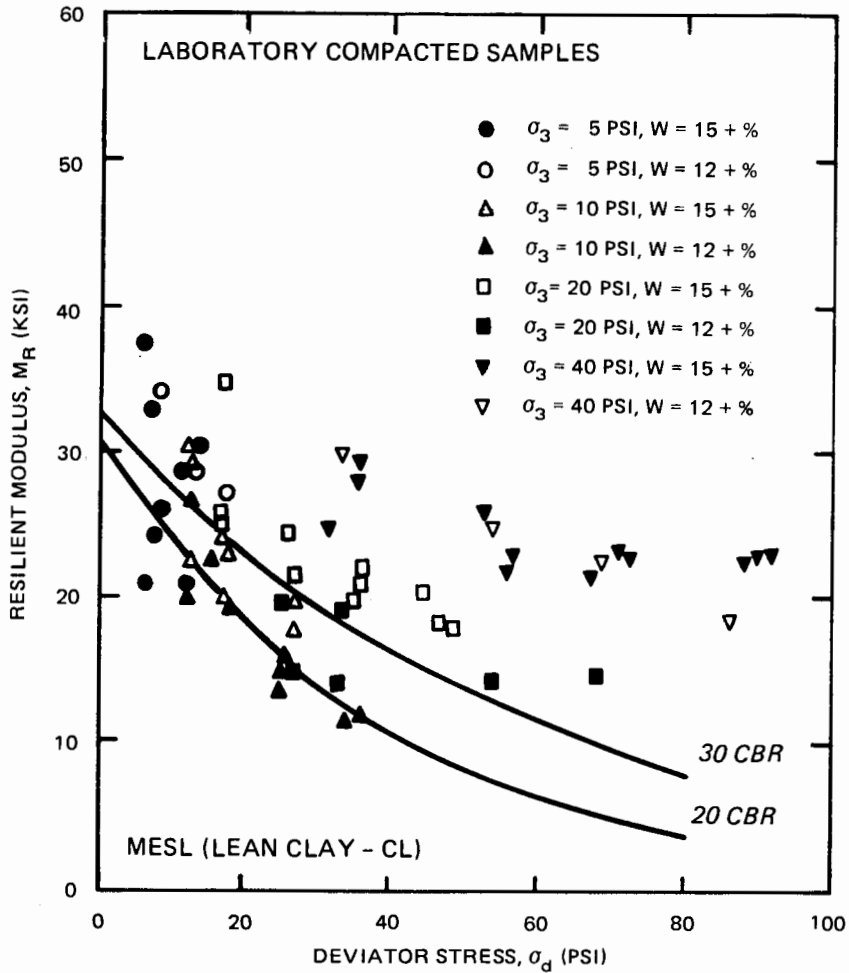


Figure 17. Resilient modulus data for lean clay used in MESL construction

Table 7  
Performance Calculation for Steel Fiber-Reinforced Concrete

Test	Item	Load kip	Westergaard Stress psi	Design Factor Westergaard*	Elastic Layer Stress psi	Design Factor- Elastic Layer**
Keyed longitudinal joint study	5	360	1,100	1.139	962	0.977
Keyed longitudinal joint study	5	166	1,617	0.775	1,240	0.758
Structural layers	1	200	1,492	0.894	1,030	0.971
Structural layers	1	240	1,790	0.894	1,240	0.968
Structural layers	2	200	2,371	0.562	995	1.005
Structural layers	2	240	2,845	0.492	1,190	0.882

\*  $DF_W = \frac{\text{modulus of rupture}}{0.75 \times \text{Westergaard calculated stress}}$

\*\*  $DF_{EL} = \frac{\text{modulus of rupture}}{\text{elastic layer calculated stress}}$

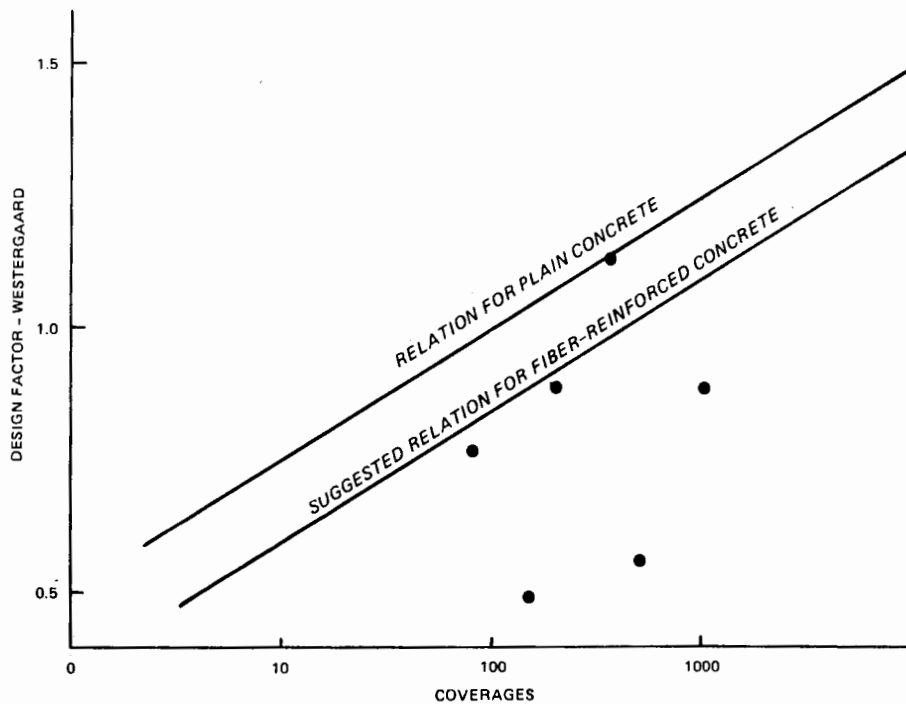


Figure 18. Steel fiber-reinforced concrete performance criteria using Westergaard based design factor

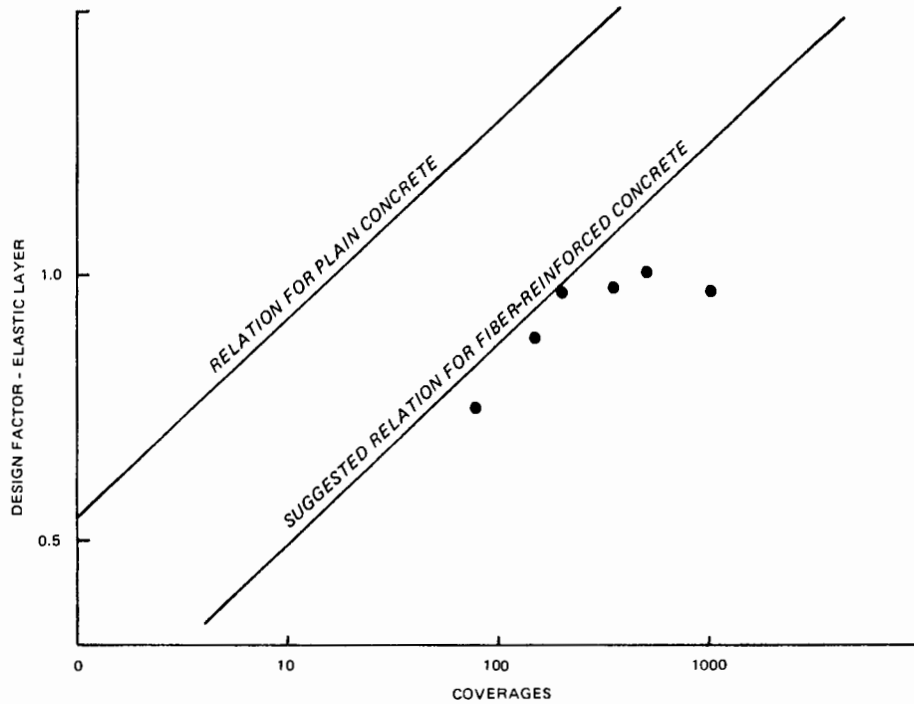


Figure 19. Steel fiber-reinforced concrete performance criteria using elastic layer based design factor

stabilized and MESL layers which are poorly modeled by the springs of the Westergaard model.

A relation in Figures 18 and 19 can now be selected for the steel fiber-reinforced concrete by drawing a line parallel to the plain concrete relation and that is a conservative bound on the data. The suggested steel fiber-reinforced concrete pavement performance criteria for the Westergaard and elastic layer models are

$$DF_W = 0.35 + 0.25 \log (\text{coverages}) \quad (11)$$

$$DF_{EL} = 0.11 + 0.38 \log (\text{coverages}) \quad (12)$$

#### OVERLAY DESIGN

Parker<sup>16</sup> also proposed a modification to the standard overlay equations<sup>10</sup> to allow design of fiber-reinforced concrete overlay as follows:

$$h_{of} = (0.75) \left\{ h_{df}^n - c \left[ \left( \frac{h_{df}}{h_{db}} \right) h_e \right]^n \right\}^{1/n} \quad (13)$$

where

$h_{of}$  = required thickness of the fibrous concrete overlay, in.

- $h_{df}$  = required thickness of an equivalent single slab of plain concrete having a flexural strength equal to the flexural strength of the fibrous concrete used for the overlay, in.  
 $h_{db}$  = required thickness of an equivalent single slab of plain concrete having a flexural strength equal to the flexural strength of the concrete in the existing pavement, in.  
 $h_e$  = thickness of the existing pavement, in.  
 $C$  = coefficient describing the condition of the existing pavement  
 $\eta$  = a power constant to describe bond condition between overlay and base pavement, equal to 1.4 for partially bonded overlays and 2.0 for unbonded overlays

The thickness terms within the radical raised to the  $1/\eta$  power all use the plain concrete performance criteria and the effect of the fiber reinforcing appears only as an increase in flexural strength. The factor 0.75 tries to account for the difference in the failure criteria between plain and fiber-reinforced concrete. In Figure 16 the ratio between the required thickness of the fiber-reinforced concrete using Parker's original criteria and the Corps of Engineers conventional concrete criteria at 5,000 coverages is 0.75.

However, Parker's proposed fiber reinforced overlay design method is no longer consistent with the design factor based criteria proposed in Equations 10 and 11. The following is the proposed method of modifying the standard overlay design equations for fiber-reinforced concrete:

$$h_{of}^{\eta} = h_{df}^{\eta} - C \left( \frac{h_{df}}{h_{dp}} h_e \right)^{\eta} \quad (14)$$

where

- $h_{of}$  = thickness of fiber-reinforced concrete overlay  
 $h_{df}$  = thickness of an equivalent new single slab of fiber-reinforced concrete using fiber-reinforced concrete performance criteria given in Equation 10 (or Equation 11 if layered elastic model is used)  
 $h_{dp}$  = thickness of an equivalent new single slab of plain concrete using the concrete performance criteria given in Equation 8 (or Equation 9 if layered elastic model is used)  
 $h_e$  = thickness of existing slab to be overlaid  
 $C$  = condition factor of existing slab with maximum value of 1.0 described in TM 5-824-3/AFM 88-6<sup>10</sup>  
 $\eta$  = power constant to describe bond condition between overlay and base slab; equal to 2.0 for unbonded overlays, 1.4 for partially bonded overlays

The term  $h_{df}/h_{dp}$  in Equation 13 essentially converts the existing plain concrete pavement thickness to an equivalent fiber reinforced thickness. This term is always less than 1.0 and reflects both the higher flexural strength of the fiber-reinforced concrete and the change in failure criteria.

The C factor further adjusts this new equivalent thickness of fiber-reinforced concrete for structural conditions such as uncracked (C = 1.0), slight cracking (C = 0.75), extensive cracking (C = 0.35), etc.

Item 3 of the keyed longitudinal joint test provides the only trafficking performance data on a fiber-reinforced concrete overlay. This item is described in detail in Table 6 and had two traffic lanes; one for a 360 kip C-5A main gear and one for a 166 kip dual tandem gear. Table 8 shows a comparison of the actual fiber reinforced overlay thickness with the thicknesses that would have been required by Equations 12 and 13 to reach the test item failure coverage levels. Under the C-5A traffic both equations required a thicker overlay than the actual one. This difference is due to the difficulty of selecting an appropriate C factor for the cracked base pavement. This selection is largely a matter of judgement and only very rough guidelines are provided in design manuals. For this specific instance a somewhat larger C factor would have been appropriate. As pointed out earlier in the analysis of transverse and longitudinal cracking, partially bonded overlays are not a good solution in overlaying badly cracked pavements such as this one.

The traffic lane for the 166 kip dual tandem gear was over an uncracked base pavement so the C factor was 1.0. Equation 13 required a thickness of 0.1 in. thicker than the actual overlay and Equation 12 required a thickness 0.6 in. thinner than the actual overlay.

Equation 13 requires somewhat thicker overlays than Parker's original Equation 12. The general lack of data and the unconservative prediction of Equation 12 for the dual tandem traffic suggest that the more conservative Equation 13 should be used in lieu of Parker's Equation 12.

## CONDITIONS AND RECOMMENDATIONS

Steel fiber-reinforced concrete pavements can be designed and built to provide serviceable airport pavements. They result in appreciably thinner pavements than plain concrete for similar load carrying capacity and may find particular value where overlays are needed but at the same time change to an existing grade must be kept as small as possible.

Table 8  
Comparison of Overlay Design Equations and Item 3 Performance

	Traffic Lane	
	C-5A	Dual Tandem
1. Traffic coverages at failure	2,800	950
2. Base pavement thickness, $h_e$ (in.)	9.5	9.5
3. Base pavement condition when overlaid	Badly cracked	Uncracked
4. Condition factor, C	0.35	1.00
5. Design thickness plain concrete, $h_{dp}$ , Equation 8 (in.)	12.2	13.3
6. Design thickness fiber reinforced, $h_{df}$ , Equation 8 (in.)*	9.3	10.1
7. Design thickness fiber reinforced, $h_{df}$ , Equation 10 (in.)	8.4	9.1
8. Required overlay thickness, $h_{of}$ , Equation 12 (in.)	5.7	3.8
9. Required overlay thickness, $h_{of}$ , Equation 13 (in.)	6.9	4.5
10. Actual overlay thickness, $h_{of}$ , (in)	4.4	4.4

\* For use in Equation 12, only higher flexural strength of fiber-reinforced concrete used in calculating design factor in Equation 8. No account for difference in failure criteria between plain and fiber reinforced concrete as represented by Equation 10.

Steel fiber-reinforced concrete pavement design procedures should be retained in TM 5-824-3,<sup>10</sup> "Rigid Pavements for Airfields Other Than Army," and added to TM 5-822-6,<sup>8</sup> "Engineering and Design, Rigid Pavements for Roads, Streets, Walks, and Open Storage Areas," and TM 5-809-12,<sup>9</sup> "Concrete Floor Slabs on Grade Subjected to Heavy Loads." Guidance for steel fiber-reinforced concrete should be added to TM 5-822-7,<sup>7</sup> "Standard Practice for Concrete Pavements."

Permanent early-age slab curl with associated corner breaks and occasional center-slab longitudinal cracking and cracking over dowel bar ends is a major problem with in-service steel fiber-reinforced concrete airfield pavements. The most likely cause of this curling is differential volume change due to autogenous shrinkage. Limiting slab dimensions to those shown in Table 4 will avoid or at least minimize this problem. Additional laboratory and field testing should examine volume change characteristics of steel fiber-reinforced concrete to develop better guidance on allowable slab size.

The Federal Aviation Administration<sup>19</sup> should publish designs and construction guidance for steel fiber reinforced concrete in either AC 150/5230-6C "Airport Pavement Design and Evaluation" or in a separate document.

Saw cut contraction joints for steel fiber-reinforced concrete should be cut a minimum of one-third of the slab thickness.

Research should be conducted to determine the actual potential for damage to jet engines from ingestion of steel fibers from the pavement surface.

Better finishing techniques are needed to provide a final surface that is durable and free from loose and protruding fibers.

The design concept for steel fiber-reinforced concrete pavements developed by Parker<sup>16</sup> and used in TM 5-824-3<sup>10</sup> appears valid. However, the improved Westergaard and the new layered elastic design factor versus coverage relationships presented in Equations 10 and 11 should be used. Additional work is still needed to develop an allowable deflection relationship for the layered elastic model. There are only limited data to support the design factor and coverage relationships and additional test data are needed, particularly at high coverage levels.

Steel fiber-reinforced concrete overlay design should use Equation 13 rather than the one in the current Army Airfield Design Manual.<sup>7</sup>

## REFERENCES

1. American Concrete Institute. 1984a. "Effect of Restraint, Volume Change and Reinforcement on Cracking of Massive Concrete," ACI 207.2R-73, ACI Manual of Concrete Practice, Part 1, Detroit, Mich.
2. \_\_\_\_\_. 1984b. "Prediction of Creep, Shrinkage, and Temperature Effects in Concrete Structures," ACI 209R-82, ACI Manual of Concrete Practice, Part 1, Detroit, Mich.
3. \_\_\_\_\_. 1984c. "State-of-the-Art Report on Fiber Reinforced Concrete," ACI 544.1R-82, ACI Manual of Concrete Practice, Part 5, Detroit, Mich.
4. Bazant, Z. P., and Wittman, F. H. 1982. Creep and Shrinkage in Concrete Structures, Wiley, New York.
5. Burns, C. D. 1974. "Comparative Performance of Structural Layers in Pavement Systems: Design, Construction, and Behavior Under Traffic of Pavement Test Sections," Technical Report S-74-8, Vol I, US Army Engineer Waterways Experiment Station, Vicksburg, Miss.
6. Grau, R. W. 1972. "Strengthening of Keyed Longitudinal Construction Joints in Rigid Pavements," Miscellaneous Paper S-72-43, US Army Engineer Waterways Experiment Station, Vicksburg, Miss.
7. Headquarters, Department of the Army. 1975. "Standard Practice for Concrete Pavements," TM 5-822-7/AFM 88-6, Chap. 8, Washington, DC.
8. \_\_\_\_\_. 1977a. "Engineering and Design; Rigid Pavements for Roads, Streets, Walks, and Open Storage Areas," TM 5-822-6/AFM 88-7, Chap. 7, Washington, DC.
9. \_\_\_\_\_. 1977b. "Concrete Floor Slabs on Grade Subjected to Heavy Loads," TM 5-809-12/AFM 88-3, Chap. 15, Washington, DC.
10. \_\_\_\_\_. 1979. "Rigid Pavements for Airfields Other Than Army," TM 5-824-3/AFM 88-6, Chap. 3, Washington, DC.
11. Jackson, R. D. 1984. "Improved Surfacing Materials for Tracked Vehicular Traffic," Technical Report GL-84-7, US Army Engineer Waterways Experiment Station, Vicksburg, Miss.
12. Miller, A. L. 1958. "Warping of Reinforced Concrete Due to Shrinkage," Journal, American Concrete Institute, Vol. 54, No. 11, Detroit, Mich.
13. Morse, D. C., and Williamson, G. R. 1977. "Corrosion Behavior of Steel Reinforced Concrete," Technical Report M-217, US Army Construction Engineering Research Laboratory, Champaign, Ill.
14. Neville, A. M. 1973. Properties of Concrete, 2nd ed., Wiley, New York.

15. Parker, Frazier. 1972. "Construction of Fibrous Reinforced Concrete Overlay Test Slabs Tampa International Airport, Florida," Miscellaneous Paper S-77-44, US Army Engineer Waterways Experiment Station, Vicksburg, Miss.
16. \_\_\_\_\_. 1974. "Steel Fibrous Concrete for Airport Pavement Applications," Technical Report S-74-12/FAA-RD-74-31, US Army Engineer Waterways Experiment Station, Vicksburg, Miss.
17. Rollings, Raymond S. 1980. "Comments on Rigid Pavement Airfield Design Manual, TM 5-824-3, August 1979," Memorandum for the Record, US Army Engineer Waterways Experiment Station, Vicksburg, Miss.
18. Schrader, E. K., and Lankard, D. R. 1983. "Inspection and Analysis of Curl in Steel Fiber Reinforced Concrete Airfield Pavements," Bekaert Steel Wire Corp., Irving, Tex.
19. US Department of Transportation. 1978. "Airport Pavement Design and Evaluation," Advisory Circular AC 150/5230-6C, Washington, DC.
20. US Department of Transportation, Federal Aviation Administration. 1980. "Procedure for Condition Survey of Civil Airports," FAA-RD-80-55, Washington, DC.
21. Waddell, J. J. 1974. Concrete Construction Handbook, 2nd ed. McGraw-Hill, New York.
22. Williamson, G. R. 1975. "Technical Information Pamphlet on Fibrous Concrete Overlays-Fort Hood Project," Technical Report M-147, US Army Engineer Construction Engineering Research Laboratory, Champaign, Ill.
23. Wu, George Y. 1985. "Performance of Fiber-Reinforced Concrete Pavements at Commerical Airfields," Technical Memorandum M-53-84-08, US Naval Civil Engineering Laboratory, Port Hueneme, Calif.
24. Yoder, E. J., and Witczak, M. W., 1975. Principles of Pavement and Design, 2nd ed., Wiley, New York.